ULB UNIVERSITÉ LIBRE DE BRUXELLES

Bruface Brussels Faculty of Engineering

VUB VRIJE UNIVERSITEIT BRUSSEL

A frequency domain approach to data-driven control

Marc Berneman

Master thesis submitted under the supervision of
Prof. Dr. Ir. Rik Pintelon

the co-supervision of
Prof. Dr. Ir. John Lataire

in order to be awarded the Degree of
Master of Science in Electrical Engineering
major in Measuring, Modeling and Control

Academic year
2019 – 2020

Title: A frequency domain approach to data-driven control

Marc Berneman: Marc Berneman
Master of Science in Electrical Engineering – major in Measuring, Modeling and Control
Academic year: 2019 – 2020

Abstract

Bla bla bla

Keywords: data-driven controller tuning; model reference control; Frequency domain approach; Nonparametric; Frequency response function

Table of Contents

List of Abbreviations

CT	Continuous-time
DFT	Discrete Fourier transform
DT	Discrete-time
FD	Frequency domain
FRF	Frequency response function
IDFT	Inverse discrete Fourier transform
LPM	Local Polynomial Method
LTI	Linear time-invariant
TD	Time domain
ZOH	Zero-order hold

Chapter 1
Introduction

Explain what nonparametric estimates are

Explain shortly what model reference control is

Explain that behind data-driven there is actually a nonparametric estimate of the FRF, which means that there still is a model hidden in the math

Explain that you can use advanced frequency domain methods to improve on the method

Chapter 2
Preliminaries

2.1 Introduction

A refresher about linear time-invariant systems is given here. Afterwards, this section focuses on frequency domain methods for estimating nonparametric estimates of the frequency response function. System transients and white noise are analysed in the frequency domain. Finally, this chapter ends with some advanced methods to suppress transients and noise in the estimate of the frequency response function.

2.2 LTI systems

Linear time-invariant (LTI) systems can be represented in different ways. In this work, we will use the transfer function representation for single-input single-output (SISO) systems.

$$G(\Omega) = \frac{B(\Omega)}{A(\Omega)}$$

with

$$\Omega = \begin{cases} s & \text{if working in continuous-time (CT)} \\ z^{-1} & \text{if working in discrete-time (DT)} \end{cases}$$

and $B(\Omega)$ and $A(\Omega)$ being polynomials in Ω. For now, we will keep our focus on CT systems. In CT, the output of this system is given by

$$y(t) = \mathcal{F}^{-1}\{Y(j\omega)\} = \mathcal{F}^{-1}\{G(j\omega)U(j\omega)\} = \mathcal{F}^{-1}\{G(j\omega)\mathcal{F}\{u(t)\}\}$$

With $\mathcal{F}$ and $\mathcal{F}^{-1}$ denoting the Fourier transform and inverse Fourier transform respectively.

$$\mathcal{F}\{x(t)\}\}(j\omega) = \int_{-\infty}^{+\infty} x(t)e^{-j\omega t}dt$$
$$\mathcal{F}^{-1}\{X(j\omega)\}(t) = \frac{1}{2\pi}\int_{-\infty}^{+\infty} X(j\omega)e^{j\omega t}d\omega$$

Because a convolution is the time domain (TD) becomes a multiplication in the frequency domain (FD), the output in the FD is simply found my doing a multiplication.

$$\boxed{Y(j\omega) = G(j\omega)U(j\omega)} \tag{2.1}$$

2.3 Single sine excitations

Assume that the input $u(t)$ of the system is a complex exponential with a single frequency.

$$u(t) = e^{j(\omega_u t+\phi)}$$

In the FD this becomes

$$U(j\omega) = 2\pi e^{j\phi}\delta(\omega - \omega_u)$$

With δ denoting the Dirac delta function. Using (2.1) gives the output in the FD is

$$Y(j\omega) = 2\pi|G(j\omega_u)|e^{j(\phi+\angle G(j\omega_u))}\delta(\omega - \omega_u)$$

Going back to the TD we find

$$y(t) = |G(j\omega_u)|e^{j\angle G(j\omega_u)}e^{j(\omega_u t+\phi)} = |G(j\omega_u)|e^{j\angle G(j\omega_u)}u(t)$$

Since the system is linear and real, this result can be used to calculate the output of the system if the input is a cosine wave.

$$u(t) = \cos(\omega_u t + \phi) = \frac{e^{j(\omega_u t+\phi)} + e^{-j(\omega_u t+\phi)}}{2}$$

After a brief calculation, the output is found to be given by

$$\boxed{y(t) = |G(j\omega_u)|\cos(\omega_u t + \angle G(j\omega_u) + \phi)}$$

To summarize, if the input of a system is a sine wave, then the output will be a sine wave with the same frequency, but with a different phase and amplitude determined by the value of the transfer function at that frequency.

2.4 Discrete Fourier transform

In practice, using the Fourier transform is not practical as it requires an infinite amount of data and an infinite resolution to compute. The discrete Fourier transform (DFT) solves both of these problems.

The DFT of a sequence $x(n)$, $n = 0, 1, \ldots, N-1$ is defined as

$$X(k) = \text{DFT}\{x(n)\} = \sum_{n=0}^{N-1} x(n)e^{-j2\pi kn/N}, \quad k \in \mathbb{Z}$$

$X(k)$ is periodic with period N, so k is usually confined to $k = 0, 1 \ldots, N-1$. The inverse DFT (IDFT) is defined in a similar way.

$$x(n) = \text{IDFT}\{X(k)\} = \frac{1}{N}\sum_{k=0}^{N-1} X(k)e^{j2\pi kn/N}, \quad n \in \mathbb{Z}$$

2.5 Perfect reconstruction

The question now is: under what conditions can we perfectly reconstruct a CT signal $x(t)$ from a DT measurement?

$$x_d(n) = x(nT_s)\,, \quad n = 0, \ldots, N-1$$

It is simpler to see when this is the case by working in the FD. The question then becomes: under which conditions does the DFT of $x_d(n)$ contain the same information as the Fourier transform of $x(t)$?

Periodicity First, as the DFT has a limited spectral resolution, the Fourier spectrum of the continuous signal must also be discrete. This is the case when the CT signal is periodic. If the CT signal has a period T

$$x(t) = x(t+T) \quad \forall t$$

then the Fourier spectrum of $x(t)$ will consist of Dirac delta functions with a fixed spacing between the Dirac pulses.

$$X(\omega) = \mathcal{F}\{x(t)\} = \sum_{n=-\infty}^{+\infty} c_n \delta(\omega - n\omega_0)\,, \quad \omega_0 = \frac{2\pi}{T}$$

Leakage Next, the DFT frequencies should coincide with the Dirac pulses to avoid leakage. The DFT bins k correspond to certain frequencies depending on the sampling frequency f_s and the number of samples N.

$$\omega_k = 2\pi k \frac{f_s}{N} = 2\pi k \frac{1}{NT_s} = 2\pi k \frac{1}{T_{\text{meas}}}$$

$T_{\text{meas}} = NT_s$ is the measurement time. The lowest frequency of the CT signal ω_{signal} needs to correspond to one of the DFT frequencies in order to avoid leakage.

$$\omega_{\text{signal}} = \omega_k \Rightarrow \boxed{T_{\text{meas}} = kT_{\text{signal}}}$$

In simple words: the measurement time must contain an integer number of periods of the CT signal.

Aliasing Finally, the famous Nyquist-Shannon sampling theorem states that the CT signal $x(t)$ must not contain frequency components higher than half the sampling frequency.

$$f_{\max} < \frac{f_s}{2}$$

To summarize, a CT signal is perfectly reconstructable from a sampled version of it in a limited time window if the DFT contains the same information as the CT Fourier transform. This is the case when the following conditions are met:

- The CT signal is periodic.
- The measurement time contains an integer number of periods.
- The bandwidth of the signal does not exceed half the sampling frequency.

2.6 Frequency response function estimation

If the input and output of an LTI system satisfy the conditions of perfect reconstructability, then the transfer function can be calculated at the excited frequencies. Taking the input to be a periodic single sine as before results in a sine in the output with the same frequency.

$$u(t) = \cos(\omega_u t + \phi) \Rightarrow y(t) = |G(j\omega_u)| \cos(\omega_u t + \angle G(j\omega_u) + \phi)$$

In the FD this becomes

$$Y(j\omega_u) = G(j\omega_u)U(j\omega_u)$$

Assuming that the excited frequency corresponds to one of the DFT frequencies $\omega_u = \omega_k = 2\pi k f_s/N$ and $|\omega_k| < \pi f_s$ fulfills the last 2 conditions of perfect reconstructability respectively.

$$U(j\omega_k) = \frac{2\pi}{N} U(k)\delta(\omega - \omega_k), \quad Y(j\omega_k) = \frac{2\pi}{N} Y(k)\delta(\omega - \omega_k)$$

With $U(k)$ and $Y(k)$ being the k-th DFT bin of $u_d(n)$ and $y_d(n)$ respectively. Note that the factor $\frac{2\pi}{N}$ is just a consequence of how the Fourier transform and the DFT are defined. In the end, we are interested in ratios, so this won't matter. This means that

$$Y(k) = G(j\omega_k)U(k) \tag{2.2}$$

Finally, the value of the frequency response function (FRF) at $s = j\omega_k$ can be calculated as

$$\boxed{G(j\omega_k) = \frac{Y(k)}{U(k)}}$$

2.7 Multisine excitations

Using a single sine excitations allows one to calculate the value of the FRF at one single frequency. We can make use of the linearity of LTI systems to calculate the FRF at multiple frequencies at once. This is where a multisine excitation can be useful.

$$u(t) = \sum_{k \in \mathrm{K_{exc}}} \frac{A_k}{N} \sin(\omega_k t + \phi_k), \quad \omega_k = 2\pi k \frac{f_s}{N}, \quad \mathrm{K_{exc}} \subseteq \{n \in \mathbb{Z} | 0 \leq n < N/2\}$$

In the FD this gives

$$U(k) = \frac{A_k}{2j} e^{j\phi_k}, \quad k \in \mathrm{K_{exc}}$$

By using (2.2) the output is

$$Y(k) = G(j\omega_k)\frac{A_k}{2j} e^{j\phi_k}, \quad k \in \mathrm{K_{exc}}$$

Thus, the FRF can be calculated for all $k \in \mathrm{K_{exc}}$.

$$G(j\omega_k) = \frac{Y(k)}{U(k)}, \quad k \in \mathrm{K_{exc}} \tag{2.3}$$

Magnitude choice The magnitude of the sine components A_k can be chosen by the user. This can be useful when noise occurs in a certain frequency band. More power can be attributed to this frequency band to get a better signal-to-noise ratio at those frequencies.

Phase choice The phases of the sine components ϕ_k can also be chosen by the user. A concise example is given to see what the consequences are of choosing a different phase. Two possibilities are shown here.

A linear phase multisine is the simplest case: all the sine components have the same phase

$$\phi_k = 0$$

In a random phase multisine the phases of the sine components have random phases drawn from a uniform distribution between 0 and 2π.

$$\phi_k \sim U(0, 2\pi)$$

Two multisines with the same RMS values are shown in figure 2.1. One has a linear phase, while the other has a random phase. The magnitude spectrum of both are the same. However, the linear phase multisine peaks at $t = 0$, while the power of the random phase multisine is more evenly distributed over time. This can be useful when the generator has a limited range due to saturation. Even though both signals contain the same power, the random phase multisine is less likely to saturate.

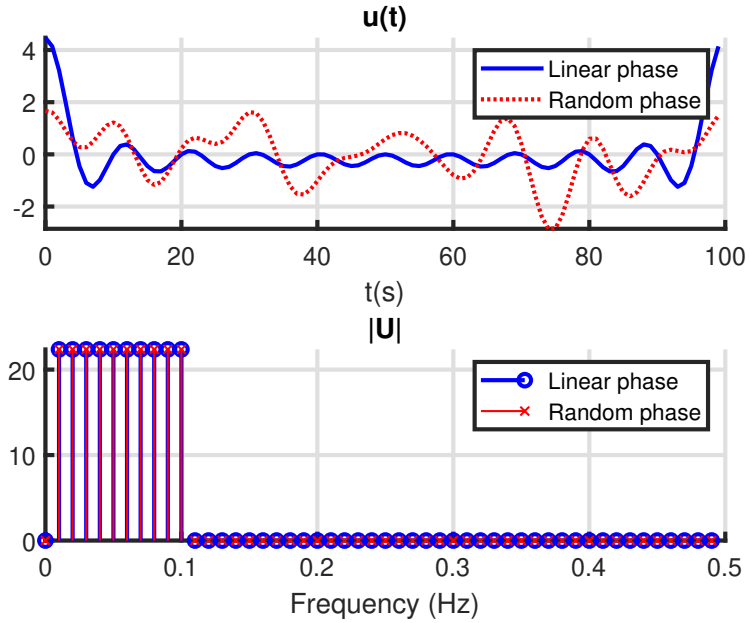

Figure 2.1 – Comparison betwee a linear phase multisine and a random phase multisine with the same RMS value.

Example Consider a DT system.

$$G(z^{-1}) = \frac{0.4097z^{-1} + 0.407z^{-2}}{1 - 1.165z^{-1} + 0.9813z^{-2}} \tag{2.4}$$

This system is excited by the random phase multisine shown in figure 2.2. The normalized frequency is the frequency divided by the sampling frequency. 0.5 represents the Nyquist frequency $f_s/2$. The steady state output of this system is shown in figure 2.3. Then the FRF can be calculated by using (2.3) at the excited frequencies. The actual FRF and calculated FRF are plotted in figure 2.4.

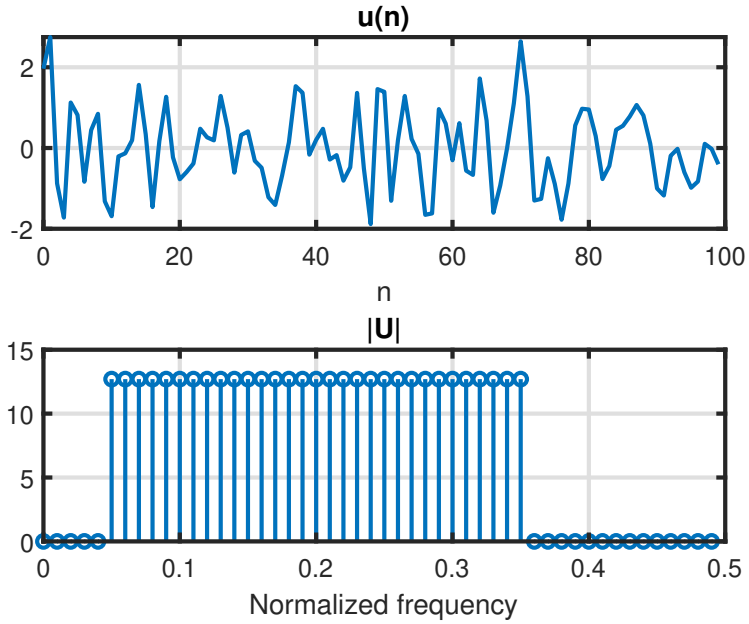

Figure 2.2 – Input of the second-order system. Random phase multisine.

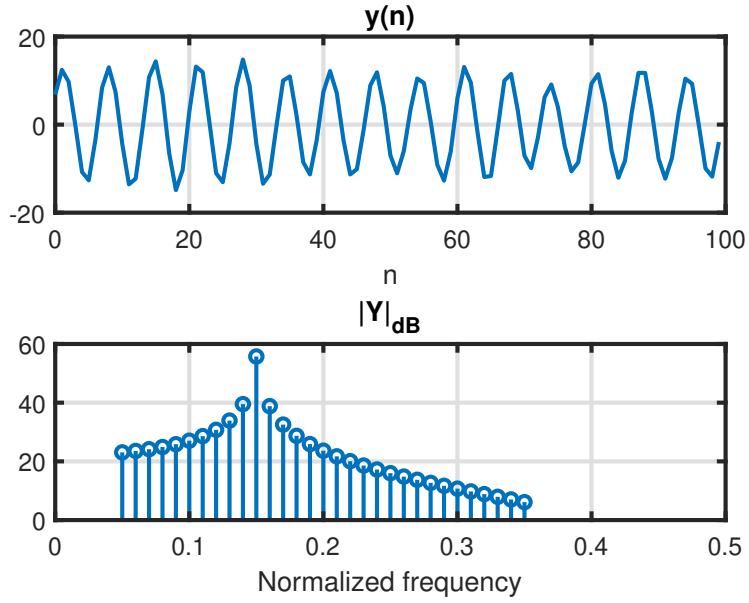

Figure 2.3 – Output of the second-order system.

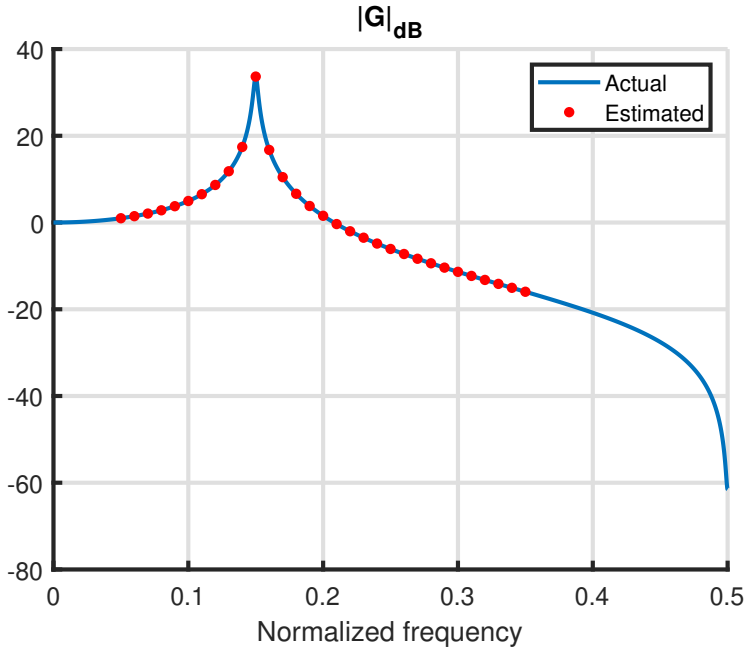

Figure 2.4 – Magnitude FRF of the second-order system and the estimated FRF at the excited frequencies using (2.3).

2.8 Measurement setups

2.8.1 Zero-order hold setup

In a lot of measurement setups, the input signal is generated digitally with a Zero-order hold (ZOH). This means that the signal is kept constant for a whole sampling period. At the sampling instances, a CT system $G(s)$ preceded by a ZOH can be modeled exactly as a DT system.

$$G_{\text{ZOH}}(z) = (1 - z^{-1})\mathcal{Z}\Big\{\mathcal{L}^{-1}\{\frac{G(s)}{s}\}|_{t=nT_s}\Big\} \tag{2.5}$$

The ZOH measurement setup is shown in figure 2.5. In this case, the actuator $G_{\text{act}}(s)$ is part of the FRF that is measured. The dynamics of the measurement device $G_y(s)$ must be calibrated perfectly ($G_y(s) = 1$) if one wants to measure the FRF from generator to output. Note that, in theory, the ZOH setup is not allowed to contain anti-alias filters.

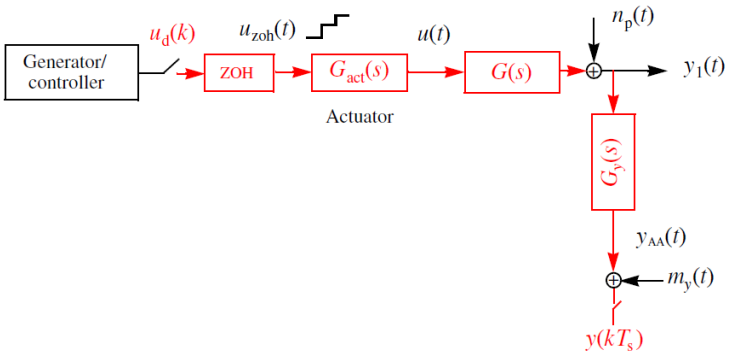

Figure 2.5 – Zero-order hold measurement setup. Red indicates which parts are modeled. Taken from [1].

Thus, if no anti-alias filter is used at the output and assuming that the actuator is perfect $G_{\text{act}}(s) = 1$, when a CT system is excited with a ZOH and is sampled, we are actually measuring the ZOH version of the FRF and not the CT FRF directly. This is bad news if we want to measure the CT FRF $G(s)$. However, this can be circumvented. When $f << f_s/2$, there isn't a big difference between the CT FRF $G(s)$ and the ZOH version of $G(s)$.

$$G(j2\pi f) \approx G_{\text{ZOH}}(e^{j2\pi f T_s}) \tag{2.6}$$

So, when one wants to measure a CT FRF with a ZOH setup, care must be taken to stay within the region where this approximation holds. This can be accomplished by making sure that the highest excited frequency in the input signal is well below the sampling frequency of the measurement setup.

$$f_{\max} << f_s/2$$

Example Consider a second order system.

$$G(s) = \frac{\omega_0^2}{s^2 + 2\zeta\omega_0 s + \omega_0^2} \text{ with } \omega_0 = 2\pi 0.3[\text{rad}/s] \text{ and } \zeta = 0.01$$

Applying the ZOH transformation (2.5) to this system with $f_s = 2$Hz results in the DT system that was used in previous examples (2.4). The magnitude FRF of both the CT system and the ZOH version of it are plotted in figure 2.6. Notice that the DT system has a periodic FRF while the CT system does not. Moreover, at the low frequencies, both FRF overlap. The approximation (2.6) is worse once the frequency gets close to $f_s/2$.

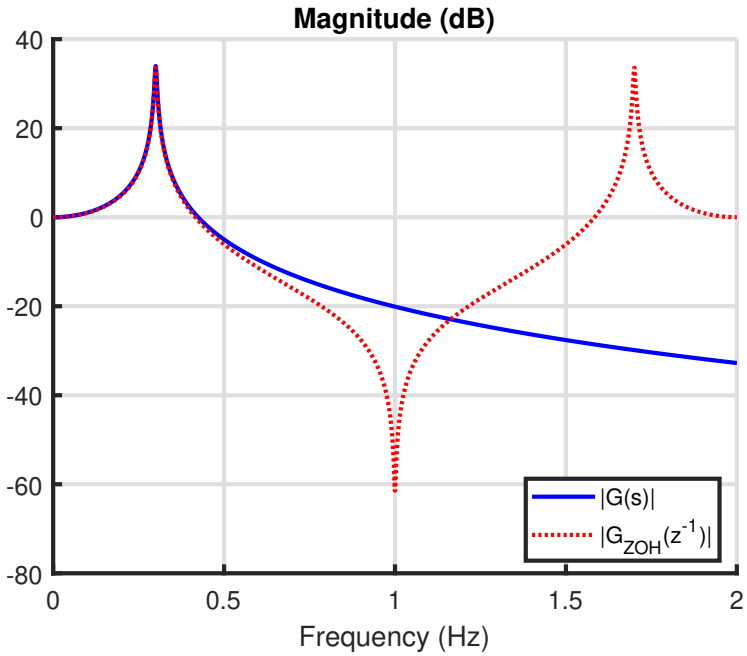

Figure 2.6 – Magnitude FRF of the second-order system and the magnitude FRF of the ZOH version of it with $f_s = 2$Hz.

2.8.2 Band-limited setup

Even if you use a high sampling frequency f_s, the actuator dynamics will still influence the measurement of the FRF when using a ZOH setup. This is not an issue when a band-limited setup is used. The band-limited setup is shown in figure 2.7. In a band-limited setup, the input to the system can still be generated by a ZOH. But the input to the system must be measured and an anti-alias filter must be used to avoid aliasing. By measuring the input to the system, the dynamics of the actuator won't be part of the FRF estimate. The output of the system must also go through an anti-alias filter before being measured. A relative calibration is needed if one wants to measure the FRF from the input to the output. Concretely this means that the anti-alias filters must be equal to each other.

$$G_u(s) = G_y(s)$$

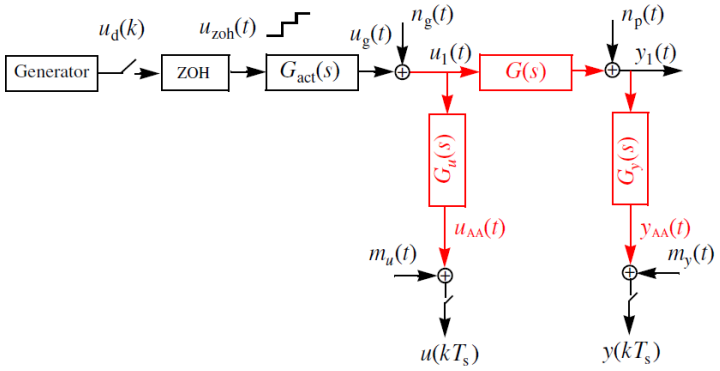

Figure 2.7 – Band-limited measurement setup. Red indicates which parts are modeled. Taken from [1].

2.9 System transients

The first condition of perfect reconstructability (periodicity) implies that the signal has been repeating forever until now and will repeat forever in the future. This is not realistic; when a system is excited, the excitation must have started somewhere in the past and must end at some point in the future. In the example of the previous section we had briefly mentioned that the measurements were taken in steady state. Concretely, the input was applied to the system for 20 periods and only the last period was used for the analysis, thereby ensuring that the system transients have faded away. This can be quantified by calculating the RMS between the output of the p-th period and the output of the last period. This is plotted in figure 2.8. The RMS of the difference decreases exponentially. If the measurements were noisy, the RMS of the difference would decrease until the transients are below noise level, at which point the transients can be said to have faded away. In this case, the RMS of the difference reaches approximately 10^{-7} by the 20-th period, which is negligible for our purposes.

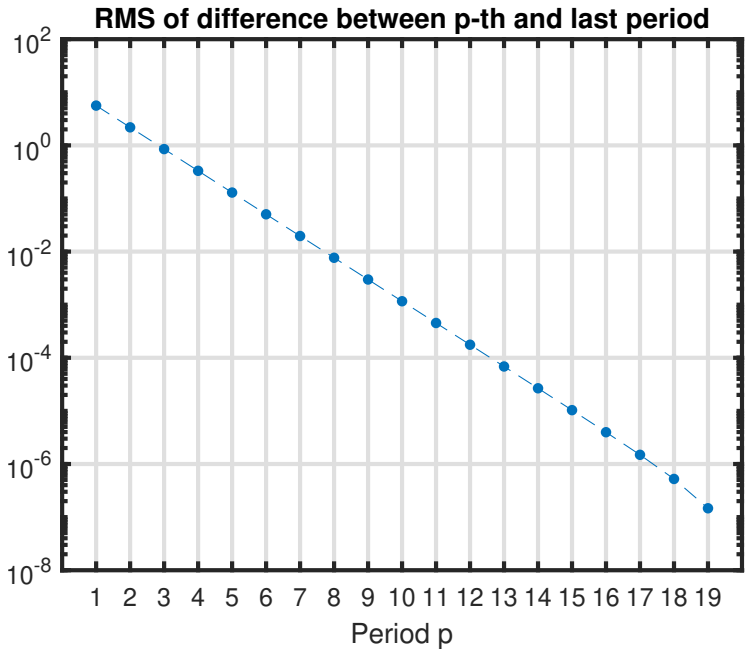

Figure 2.8 – RMS of the difference between the output of every period and the output of the last period.

It turns out that the transient term is just a rational function added on top of the steady state output spectrum.

$$\boxed{Y(k) = G(e^{-j2\pi k/N})U(k) + T(k)} \tag{2.7}$$

with

$$T(k) = \frac{I(e^{-j2\pi k/N})}{A(e^{-j2\pi k/N})}$$

This is proven for DT systems in appendix 2.A. The transient term for CT systems will be discussed afterwards.

If $u(n)$ and $y(n)$ are periodic, then $T(k) = 0$, because $I(e^{-j2\pi k/N})$ only depends on the difference between the in- and output in the current period and the in- and output in the previous period. In this case (2.7) simplifies to what we had before.

$$Y(k) = G(e^{-j2\pi k/N})U(k)$$

A key property of the transient term $T(k)$ is that it is a "smooth" function of the frequency k. This is due to the fact that it is a rational form of $e^{-j2\pi k/N}$. This property can be used to suppress the transient, as will be explained later. Another property of $T(k)$ is that its denominator is the same as the denominator of $G(e^{-j2\pi k/N})$. Therefore, the transient term will "resemble" the shape of the FRF.

CT transients Similar results can be derived for CT systems.

$$\boxed{Y(k) = G(j\omega)U(k) + T(k) + \delta(k)}$$

In this case, the numerator of $T(k)$ depends on the difference in initial conditions at $t = 0$ and $t = T = nT_s$:

$$\left[\frac{d^p y}{dt^p}(T) - \frac{d^p y}{dt^p}(0)\right] \text{ and } \left[\frac{d^p u}{dt^p}(T) - \frac{d^p u}{dt^p}(0)\right]$$

with $p \in \mathbb{N}$. An additional term $\delta(k)$ pops up. This is the alias error and it can be generated when the transient $T(j\omega)$ overextends into the aliasing frequencies $f > f_s/2$. It is present even if the signals have been low-pass filtered. Because the alias error $\delta(k)$ is also smooth, it can be grouped together with the transient term $T(k)$.

Example Again, the same second-order system (2.4) of the previous section is used. This time I'll take a look at the estimation error.

$$\begin{aligned} G_{\text{est}}(e^{-j2\pi k/N}) - G(e^{-j2\pi k/N}) &= \frac{Y(k)}{U(k)} - G(e^{-j2\pi k/N}) \\ &= \frac{G(e^{-j2\pi k/N})U(k) + T(k)}{U(k)} - G(e^{-j2\pi k/N}) \\ &= \frac{T(k)}{U(k)} \end{aligned}$$

As the magnitude spectrum of $u(n)$ is flat, the magnitude of the estimation error will be proportional to the magnitude of the transient term.

The estimation error for the FRF estimated from the first and 20th period is shown in figure 2.9. The error of the FRF calculated from the last period is around -150dB, which is negligible. In other words, there is no transient term as the data is in steady state. The error for the first period is a smooth function of the frequency and "resembles" the shape of the transfer function as expected.

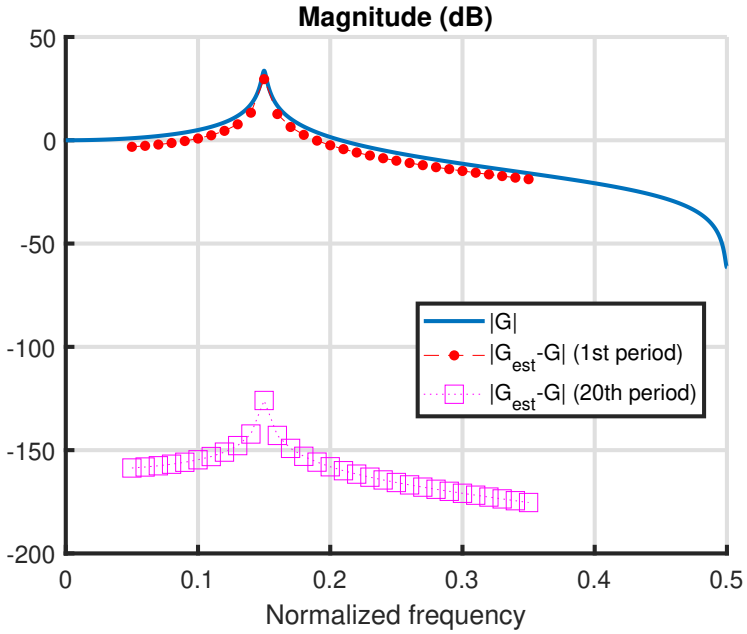

Figure 2.9 – Magnitude FRF of the second-order system and the estimation errors of the FRF at the excited frequencies using (2.3) for the data from the first period and the 20th period.

2.10 Frequency domain methods

Till now we have been treating CT and DT systems as separate cases. However, FD methods can be generalized to both CT and DT systems. There is no reason why a FD method should only work for one and not the other. To generalize these methods it is useful to define Ω to encompass both CT and DT models. Ω can either be s or z^{-1}.

$$\Omega = \begin{cases} s & \text{if working in continuous-time (CT)} \\ z^{-1} & \text{if working in discrete-time (DT)} \end{cases}$$

Thus, denoting an LTI system as $G(\Omega)$ is not specific to CT or DT systems. When the FRF is evaluated in the DFT frequencies $\omega_k = 2\pi k f_s/N$ it, is denoted Ω_k.

$$\Omega_k = \begin{cases} j\omega_k = j2\pi k f_s/N & \text{if working in continuous-time (CT)} \\ e^{-j\omega_k T_s} = e^{-j2\pi k/N} & \text{if working in discrete-time (DT)} \end{cases}$$

2.11 White noise

White noise is a random signal with a flat power spectrum. A zero-mean Gaussian sequence is white noise.

$$v(n) \sim \mathcal{N}(0, \sigma^2)$$

Let's assume that a measurement is perturbed by this white noise.

$$x(n) = x_0(n) + v(n)$$

Due to the linearity of the DFT one obtains

$$X(k) = X_0(k) + V(k)$$

Thus it is interesting to understand the properties of the DFT of this white noise sequence.

$$V(k) = \sum_{n=0}^{N-1} v(n) e^{-j2\pi kn/N}$$

It turns out that (see appendix 2.B)

$$\begin{aligned}
&\mathbb{E}\{V(k)\} = 0 \\
&\mathbb{E}\{|V(k)|^2\} = N\sigma^2 \\
&\mathbb{E}\{V^2(k)\} = 0 \text{ if } \mathrm{mod}(2k, N) \neq 0
\end{aligned}$$

2.12 Periodic signals

What happens to the DFT spectrum when we apply a signal periodically? Let's assume that we have a sequence $\tilde{x}(n)$ of length N with corresponding DFT

$$\tilde{X}(k) = \sum_{n=0}^{N-1} \tilde{x}(n) e^{-j2\pi kn/N}$$

Now, the sequence $\tilde{x}(n)$ will be repeated one more time to obtain a sequence of length $2N$.

$$x(n) = \begin{cases} \tilde{x}(n) & \text{if } 0 \leq n < N-1 \\ \tilde{x}(n-N) & \text{if } N \leq n < 2N-1 \end{cases}$$

The DFT of $x(n)$ is then given by

$$\begin{aligned}
X(k) &= \sum_{n=0}^{2N-1} \tilde{x}(n) e^{-j2\pi kn/(2N)} = \sum_{n=0}^{N-1} \tilde{x}(n) e^{-j2\pi kn/(2N)} + \sum_{n=N}^{2N-1} \tilde{x}(n-N) e^{-j2\pi kn/(2N)} \\
&= \sum_{n=0}^{N-1} \tilde{x}(n) e^{-j2\pi kn/(2N)} + \sum_{n=0}^{N-1} \tilde{x}(n) e^{-j2\pi kn/(2N)} e^{-j2\pi k/2} \\
&= \sum_{n=0}^{N-1} \tilde{x}(n) e^{-j2\pi kn/(2N)} (1 + e^{-j2\pi k/2})
\end{aligned}$$

Evaluating this in $2k$ and $2k+1$ gives

$$\begin{aligned}
X(2k) &= 2\tilde{X}(k) \\
X(2k+1) &= 0
\end{aligned}$$

Thus, the even DFT lines will contain the information of $X(k)$ and the uneven DFT lines will be zero.

This result can be generalized to a signal that is repeated for P times.

$$\boxed{x(n) = \tilde{x}(\mathrm{mod}(n, P)) \Rightarrow X(kP + r) = \begin{cases} P\tilde{X}(k) & \text{if } r = 0 \\ 0 & \text{if } r = 1, \ldots, P-1 \end{cases}}$$

Example A random phase multisine ($N = 40$) is created where the 3 lowest DFT bins are excited with an RMS value of 1. This signal is repeated $P = 3$ times. The repeated signal is plotted in the TD and the FD in figure 2.10. It can be seen that in the periodic signal there are $P - 1 = 2$ non-excited lines in between the excited lines.

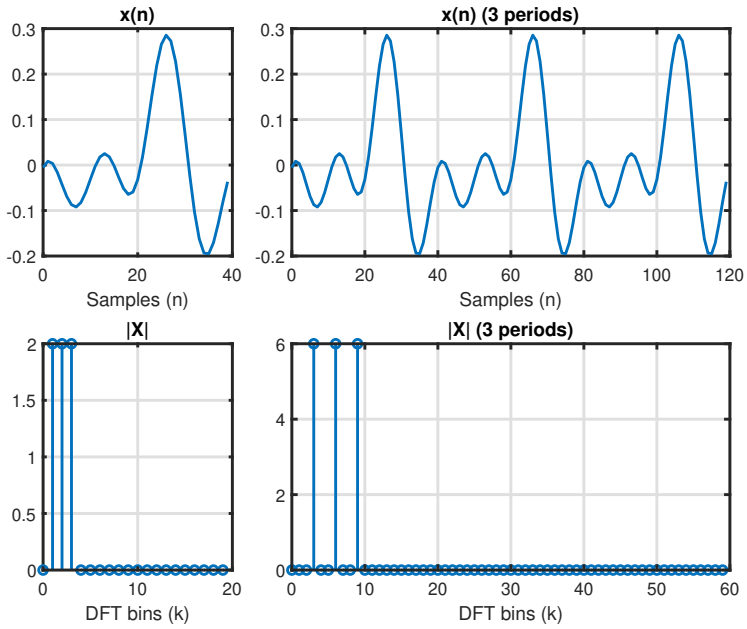

Figure 2.10 – A multisine is repeated 3 times.

2.13 Transient suppression

In section 2.9 it was shown that transients in the output will negatively impact the quality of the FRF estimate. However, there are multiple ways to suppress these transients. The most obvious way is to wait for the system to enter steady state and to only start measuring once the transients have faded away. This is exactly what was done in the example of section 2.9 (see figure 2.9). There are also ways to suppress the transient without throwing away the measurements that are not in steady state. 3 of them will be discussed:

- Windowing
- Parametric estimation
- The local polynomial method

2.13.1 Windowing

There are many possible windows that one can choose from. The Hann window is a popular one.

$$w(n) = \frac{1}{2}[1 - \cos(\frac{2\pi n}{N})], \quad n = 0, \ldots, N-1 \tag{2.8}$$

The windowed input and output are then given by

$$u_w(n) = w(n)u(n) \text{ and } y_w(n) = w(n)y(n)$$

A multiplication in the TD becomes a convolution in the FD.

$$U_W(k) = W(k) * U(k) \text{ and } Y_W(k) = W(k) * Y(k)$$

with $W(k) = N\left[\frac{1}{2}\delta(k) - \frac{1}{4}\delta(k+1) - \frac{1}{4}\delta(k-1)\right]$. The windowed estimate of the FRF is then given by

$$G_W(\Omega_k) = \frac{Y_W(k)}{U_W(k)} \tag{2.9}$$

Let's now see why windowing will reduce the effect of the transient.

$$Y_W(k) = W(k) * (G(\Omega_k)U(k) + T(k))$$

For the first term the following approximation can be made:

$$W(k) * [G(\Omega_k)U(k)] \approx G(\omega_k)[W(k) * U(k)] = G(\omega_k)U_W(k)$$

Hereby it is assumed that $G(\Omega_{k-1}) \approx G(\Omega_k) \approx G(\Omega_{k+1})$. In other words, $G(\Omega)$ is flat around Ω_k. (2.9) then becomes

$$G_W(\Omega_k) \approx G(\Omega_k) + \frac{T_W(k)}{U_W(k)}$$

The trick now is to use the property that $T(k)$ is a smooth function of the frequency. Let's assume that $T(k)$ can be captured locally by a second order polynomial.

$$T(k) = ak^2 + bk + c$$

Windowing $T(k)$ gives

$$T_W(k) \propto 2T(k) - T(k+1) - T(k-1) = -2a$$

This is a bit like taking the second derivative, which suppresses the transient.

Example The DT system (2.4) is taken again. The same input as in figure 2.2 is used. The estimation error of the FRF with and without windowing is shown in figure 2.11. Windowing gives better results, except near the resonance frequency. This is because the approximation that $G(\Omega)$ is flat does not hold in this region.

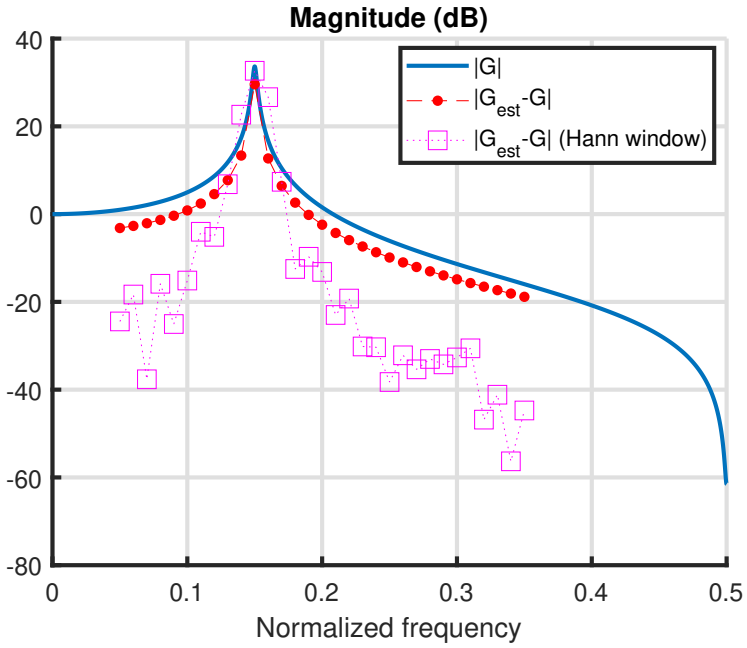

Figure 2.11 – Comparison of FRF estimation error without and with Hann windowing.

2.13.2 Parametric estimation

Until now, only non-parametric estimates of the FRF were discussed. Unlike line-fitting, where one is interested in the slope and offset of the line, the non-parametric estimate does no such thing. The result of the non-parametric estimate is the FRF estimate at every excited frequency. However, in a sense there are still parameters: these are the FRF estimates at every frequency bin $k \in \mathrm{K_{exc}}$.

The TF of the system is however still given by a rational function. The coefficients of this rational function can be estimated. The transient term is also a rational function and the parameters describing it can also be included in the estimation.

$$Y(k) = G(\Omega_k)U(k) + T(k)$$

Using $G(\Omega_k) = \frac{B(\Omega_k)}{A(\Omega_k)}$ and $T(k) = \frac{I(\Omega_k)}{A(\Omega_k)}$ the expression above can be rewritten as

$$A(\Omega_k)Y(k) - B(\Omega_k)U(k) - I(\Omega_k) = 0 \tag{2.10}$$

$A(\Omega_k)$ is a polynomial of order n_a and $B(\Omega_k)$ is a polynomial of order n_b. (2.18) is an explicit formula for $I(\Omega_k)$. It is easy to see that $I(\Omega_k)$ is a polynomial of order n_I with

$$n_I = \max(n_a, n_b) - 1$$

For CT systems, there is also an alias error on top of the transient term. These errors can also be captured well by a polynomial. Grouping the alias error together with the $I(\Omega_k)$ results in [2, Section 6.3.2.3]

$$n_I \geq \max(n_a, n_b)$$

After a bit of calculations, (2.10) can be turned into

$$\begin{bmatrix} \vdots & & \vdots & \vdots & & \vdots & \vdots & & \vdots \\ Y(k) & \dots & Y(k)\Omega_k^{n_a} & U(k) & \dots & U(k)\Omega_k^{n_b} & 1 & \dots & \Omega_k^{n_I} \\ \vdots & & \vdots & \vdots & & \vdots & \vdots & & \vdots \end{bmatrix} \begin{bmatrix} a_0 \\ \vdots \\ a_{n_a} \\ -b_0 \\ \vdots \\ -b_{n_b} \\ -i_0 \\ \vdots \\ -i_{n_I} \end{bmatrix} = 0$$

This can be solved by calculating the right null-space of the first matrix. The coefficients i_p will capture the transient. Note that the null space is empty if the measurements are noisy. We won't go into these details in this work, so interested reader is referred to [3].

Example Again, the DT system (2.4) is used with the same input shown in figure 2.2. The parameters are determined as described above. The resulting FRF estimation error is plotted in figure 2.12. Note that as a parametric representation is obtained, the FRF can be calculated at all frequencies. The error is around −300dB, which is MATLAB's precision. This means that the error is negligible and that the transient has been fully suppressed.

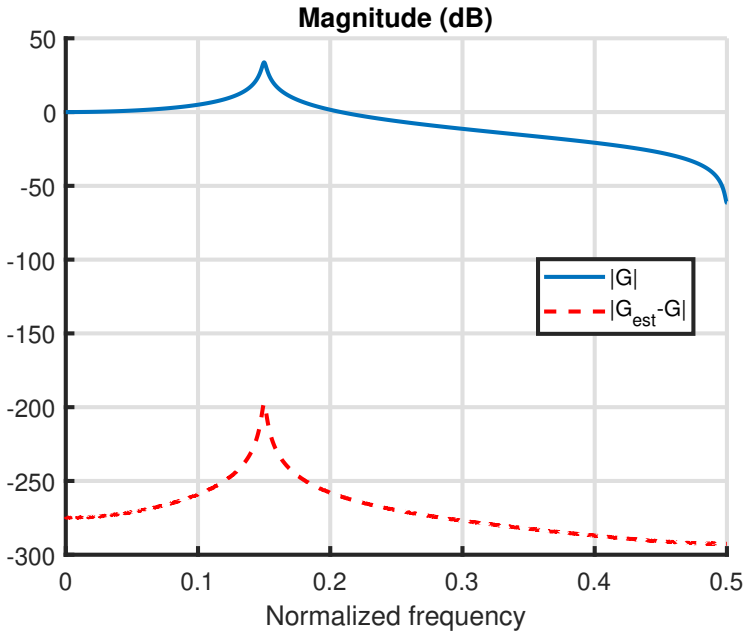

Figure 2.12 – FRF estimation error for the parametric estimation of the TF with transient terms.

2.14 Local polynomial method

The idea of the local polynomial method (LPM) is quite simple. There are multiple variants of the LPM, but here we will focus on the robust LPM for periodic excitations. More information about all the variants of the LPM can be found in [2, Chapter 7].

2.14.1 Response of a system excited by a periodic input

For the robust LPM for periodic signals to work, at least $P = 2$ periods must be measured. Let's assume for the sake of simplicity that the input $\tilde{u}(n)$ is noiseless and in steady state. $\tilde{u}(n)$ is applied P consecutive times to the system.

$$u(n) = \tilde{u}(\mathrm{mod}(n, P)), \quad n = 0, 1, \ldots, NP - 1$$

The spectrum of $u(n)$ is

$$U(kP + r) = \begin{cases} P\tilde{U}(k) & \text{if } r = 0 \\ 0 & \text{if } r = 1, \ldots, P - 1 \end{cases} \tag{2.11}$$

It will resemble the spectrum shown in figure 2.10. Assuming that the output is perturbed by additive noise, the output spectrum is given by

$$Y(kP + r) = G(kP + r)U(kP + r) + T(kP + r) + N_y(kP + r)$$

$T(kP + r)$ is the transient term that arises from the fact that the system might not be in steady state. $N_y(kP + r)$ is additive noise that is added to the output. It can either be white noise (see section 2.11) or filtered white noise. Using (2.11), we can be more specific about the output spectrum.

$$Y(kP + r) = \begin{cases} G(kP)U(kP) + T(kP) + N_Y(kP) & \text{if } r = 0 \\ T(kP + r) + N_Y(kP + r) & \text{if } r = 1, \ldots, P - 1 \end{cases}$$

Example The system (2.4) is excited with the signal shown in figure 2.10. The output is perturbed by Gaussian white noise with a standard deviation of 0.005. The input and output spectra are plotted in figure 2.13. The output spectrum at the DFT lines 3, 6 and 9 are dominated by the $G(kP)U(kP)$ term. There is a peak around the 18-th DFT line that corresponds to the transient term T. The 18-th DFT line corresponds to the normalized frequency $18/(NP) = 18/120 = 0.15$, which corresponds to the normalized resonance frequency of the system (see figure 2.12 for example). This is to be expected as the transient resembles the shape of the transfer function. Finally, after the 30-th DFT bin, the noise terms N_Y dominate the output.

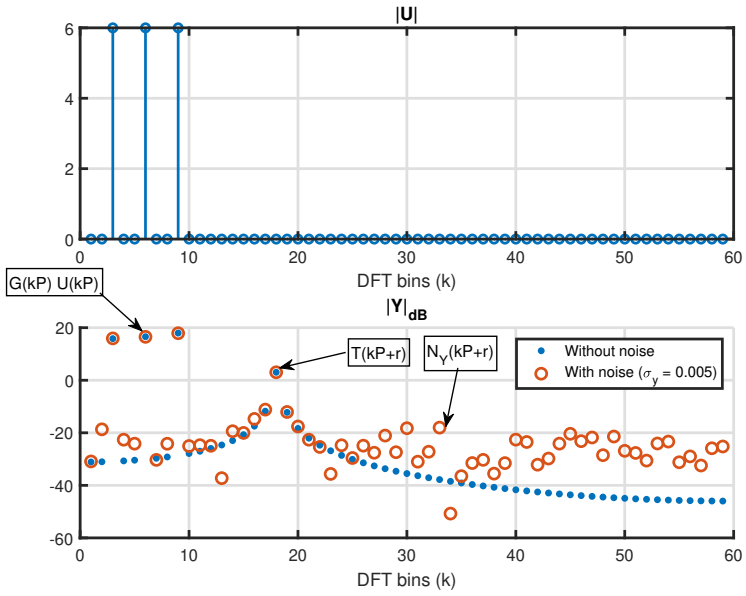

Figure 2.13 – Input and output of the DF system (2.4)

2.14.2 Algorithm

Now we can finally discuss the algorithm of the robust LPM. The idea is to estimate the contribution of the transient term at the excited frequencies by estimating it from the non-excited frequencies. To this end, we will work in a window around every excited DFT bin. In the case of the previous example, the excited bins are k = 1, 2 and 3. Two parameters must be chosen by the user. The first one is the windowsize $2n$. We must use n unexcited bins before and after kP.

Example $k = 3$, $P = 3$, $n = 4$. We are working in a window around $Y(kP) = Y(9)$. We must use 4 unexcited bins before and after 9.

$$Y(9 + r_i) \text{ with } r_i = -5, -4, -2, -1, 1, 2, 4, 5$$

For every one of the unexcited lines the following holds

$$Y(kP + r_i) = T(kP + r_i) + N_Y(kP + r_i)$$

The transient term can be modeled as a polynomial in r. This is because the transient is a smooth function of the frequency. The order of the polynomial R is the second parameter that the user can choose.

$$T(kP + r) \approx T(kP) + \sum_{s=1}^{R} t_s(k) r^s$$

We can then find the polynomial of best fit through the points $Y(kP + r_i)$

Example continued Putting all the $Y(9 + r_i)$ into a vector and choosing $R = 2$ gives

$$\begin{bmatrix} Y(4) \\ Y(5) \\ Y(7) \\ Y(8) \\ Y(10) \\ Y(11) \\ Y(13) \\ Y(14) \end{bmatrix} = \begin{bmatrix} 1 & (-5) & (-5)^2 \\ 1 & (-4) & (-4)^2 \\ 1 & (-2) & (-2)^2 \\ 1 & (-1) & (-1)^2 \\ 1 & 1 & 1^2 \\ 1 & 2 & 2^2 \\ 1 & 4 & 4^2 \\ 1 & 5 & 5^2 \end{bmatrix} \begin{bmatrix} T(9) \\ t_1(3) \\ t_2(3) \end{bmatrix} + \begin{bmatrix} N_Y(4) \\ N_Y(5) \\ N_Y(7) \\ N_Y(8) \\ N_Y(10) \\ N_Y(11) \\ N_Y(13) \\ N_Y(14) \end{bmatrix} \longrightarrow Y_n = K_n \Theta + V_n$$

The least squares solution is given by[1]

$$\hat{\Theta} = (K_n^H K_n)^{-1} K_n^H Y_n$$

This results in an estimation of the transient term at the excited DFT bin $\hat{T}(9)$. The other terms $t_1(3)$ and $t_2(3)$ are not important.

Finally, the estimated transient term can be removed from the output spectrum at the excited DFT line.

$$\boxed{\hat{Y}(kP) = Y(kP) - \hat{T}(kP)}$$

Thus, the transient has been suppressed. The FRF can then be calculated simply as

$$\hat{G}(\Omega_k) = \frac{\hat{Y}(kP)}{U(kP)}$$

The entire procedure outlined here must be repeated for all $k \in \mathrm{K_{exc}}$.

[1] Note that calculating the solution like this results in an ill-conditioned problem. The \ operator in MATLAB solves this problem using QR-factorisation, which is better conditioned. ($\theta = K_n \backslash Y_n$)

2.14.3 Variance estimate

Having a variance estimate of the output spectrum is useful for providing uncertainty bounds. It can also be used as a nonparametric weighting in parametric identification of the system transfer function.

The residual is defined as the difference between the measured output spectrum and the predicted output spectrum.

$$\hat{V}_n = Y_n - K_n\hat{\Theta}$$

Assuming that the variance of the noise is white (flat) in the window $2n$, it can be used to estimate the variance at every $k \in \mathrm{K_{exc}}$.

$$\hat{\sigma}^2_{\hat{Y}}(kP) = \frac{1}{q^{\text{noise}}} V_n^H V_n\,, \qquad \text{with } q^{\text{noise}} = 2n - (R+1) \text{ (degrees of freedom)}$$

A proof of this is given in appendix 2.C and is based on [2, Appendix 7.B]. The reason why we must divide by the degrees of freedom q^{noise} and not by $2n$ is because $R{+}1$ parameters are estimated. This is analogous to the reason why the unbiased sample variance is calculated by dividing by the number of observations - 1 when the population mean is also estimated.

As $\hat{G}(\Omega_k) = \hat{Y}(kP)/U(kP)$, the variance of the FRF can be calculated as

$$\hat{\sigma}^2_{\hat{G}}(\Omega_k) = \frac{\hat{\sigma}^2_{\hat{Y}}(kP)}{|U(kP)|^2} \tag{2.12}$$

2.14.4 Example

The robust LPM is applied to measurements from the system (2.4). This time $N = 16384$ and $P = 2$. The first $F = 5000$ frequencies are excited with a random phase multisine with an RMS value 1. White Gaussian noise is added to the output with $\sigma_y = 0.2$. 100 noise realizations are simulated and the root-mean square (RMS) error is calculated to get an idea of the effectiveness of the estimator.

$$\text{RMS}[|\hat{G} - G|](\Omega_k) = \sqrt{\frac{1}{100}\sum_{i=1}^{100} |\hat{G}^{(i)}(\Omega_k) - G(\Omega_k)|^2}$$

with $\hat{G}^{(i)}(\Omega_k)$ being the nonparametric estimate of $G(\Omega_k)$ for the i-th noise realization. The parameters used for the LPM are $R = 2$, $n = 6$ which results in $q^{\text{noise}} = 9$ degrees of freedom. To make the results more presentable, the data points are taken together in windows of size 50 and are averaged. The results are shown in figure 2.14. Not taking the transient into account is significantly worse around the resonance frequency of the system. The transient resembles the FRF of the system, which is why the error is most pronounced around the resonance frequency. However, far away from the resonance frequency, not taking the transient into account is approximately 1 dB better than using the Robust LPM. This is because transient term is below the random noise contribution. LPM uses a noisy estimate of the transient and this estimate is subtracted from the output spectrum, leading to an increased variance. Finally, the robust LPM seems to be slightly better than windowing in this simulation.

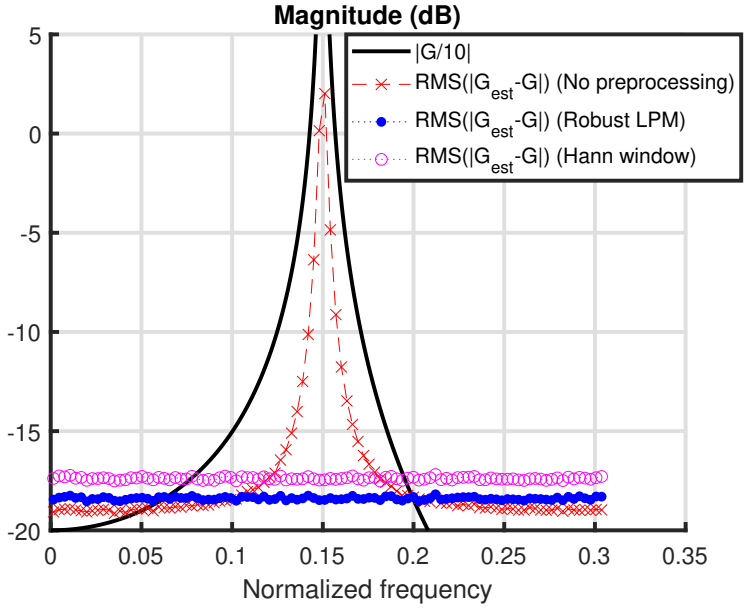

Figure 2.14 – Comparison of the RMS error for the nonparametric estimate acquired without preprocessing, with windowing and with the robust LPM. $R = 2$, $n = 6$, $q^{\text{noise}} = 9$.

2.14.5 Choice of the order and degrees of freedom

Two parameters can be chosen by the user when performing the robust LPM analysis: the order of the polynomial approximation and the degrees of freedom used to estimate the noise variance.

Order A good way to choose the order is to start at $R = 2$ and increment it in steps of two until the estimate of the variance $\hat{\sigma}^2_{\hat{G}}$ stops decreasing.

Degrees of freedom Increasing the degrees of freedom q^{noise} will increase the windowsize $2n$. This gives a better estimation of the variance. There is a trade-off however: it was assumed that the noise variance is white (flat) in the window $2n$. Thus, making the windowsize too big will result in a loss of frequency resolution. Additionally, making the windowsize $2n$ bigger means that the transient is approximated by a polynomial over a larger window. At that point it might be necessary to increase the order R of the polynomial.

2.15 Generalization

Many things were simplified until now. A few of the assumptions that were made are:

- The input is noiseless.
- White Gaussian noise noise was simulated in the example, but what if the noise is filtered white noise?
- There is no feedback from output to input.
- The input is a multisine. What about random excitations?

Each of these points will be discussed briefly.

2.15.1 Noisy input

Of course, the measurement of the input can be noisy. Thankfully, the robust LPM is also able to estimate the input noise variance for periodic excitations. Given that the input is not known perfectly, the estimate of the FRF variance (2.12) is not correct anymore. In general, the variance of an FRF estimate $\hat{G}(\Omega_k)$ can be approximated by

$$\hat{\sigma}^2_{\hat{G}}(k) = |\hat{G}(\Omega_k)|^2 \left(\frac{\hat{\sigma}^2_{\hat{Y}_k}}{|\hat{Y}_k|^2} + \frac{\hat{\sigma}^2_{\hat{U}_k}}{|\hat{U}_k|^2} - 2\text{Re}\left(\frac{\hat{\sigma}^2_{\hat{Y}_k\hat{U}_k}}{\hat{Y}_k \overline{\hat{U}_k}} \right) \right)$$

The equation above is only applicable when the excitation is periodic and when the FRF is estimated by dividing the output spectrum $Y(k)$ by the input spectrum $U(k)$. It is also possible to estimate the variance of the noise for arbitrary excitations, but different formulas must be used. [2, Section 2.6]

2.15.2 Filtered white noise

For simplicity sake, filtered white noise is defined as

$$v(n) = S(z^{-1})e(n)\,, \qquad \text{with } e(n) \sim \mathcal{N}(0, \sigma^2)$$

The power spectrum of this noise is not flat. This also means that the noise samples can be correlated over time.

$$\exists n, m \text{ with } n \neq m \text{ such that } \mathbb{E}\{v(n)v(m)\} \neq 0$$

An important consequence of filtered white noise is that there will also be noise transients in the measurements.

$$V(k) = S(\Omega_k)E(k) + T_s(\Omega_k)$$

As the input of the noise filter is random, the noise transients will never fade away. This means that when one waits long enough for the system $G(\Omega)$ to enter steady state, there will still be noise transients in the measurements. This is where the LPM can also be useful.

2.15.3 Feedback

Consider the measurement setup shown in figure 2.15. An LTI system $G(z^{-1})$ is in negative feedback and the output is perturbed by process noise.

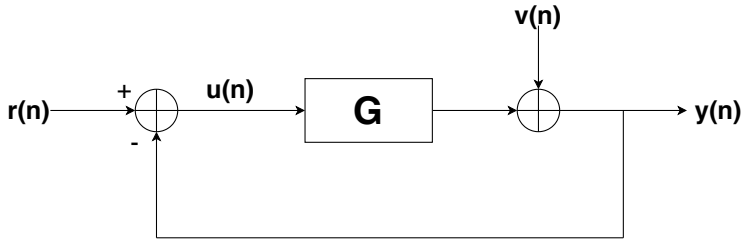

Figure 2.15 – LTI system in negative feedback with additive process noise.

The Z-transform of the output and input are given by

$$Y(z) = \frac{G}{1+G}R(z) + \frac{1}{1+G}V(z)$$
$$U(z) = \frac{1}{1+G}R(z) - \frac{1}{1+G}V(z)$$

Noise that affects the output also affects the input due to feedback. Two possibilities will be considered: $r(n)$ is a multisine and $r(n)$ is a random signal. The statistical properties of the noise are

$$\mathbb{E}\{V(k)\} = 0 \text{ and } \mathbb{E}\{|V(k)|^2\} = \sigma_v^2(k)$$

$r(n)$ is a multisine In this case we can apply multiple periods P to the system. It is assumed that enough time has passed for the transient to fade away and the noise transients will be neglected.

$$Y^{(p)}(k) = \frac{G(\Omega_k)}{1+G(\Omega_k)}R^{(p)}(k) + \frac{1}{1+G(\Omega_k)}V^{(p)}(k)$$
$$U^{(p)}(k) = \frac{1}{1+G(\Omega_k)}R^{(p)}(k) - \frac{1}{1+G(\Omega_k)}V^{(p)}(k)$$

The superscript $^{(p)}$ denotes the period of the measurement. The nonparametric FRF can then be estimated with

$$\hat{G}(\Omega_k) = \frac{\frac{1}{P}\sum_{p=0}^{P} Y^{(p)}(k)}{\frac{1}{P}\sum_{p=0}^{P} U^{(p)}(k)} \tag{2.13}$$

Taking the limit for $P \to \infty$ will allow us to establish whether this estimator is consistent.

$$\lim_{P\to\infty} \hat{G}(\Omega_k) = \frac{\mathbb{E}\{Y^{(p)}(k)\}}{\mathbb{E}\{U^{(p)}(k)\}} = G(\Omega_k)$$

The first equality applies the law of large numbers for independent experiments. And so this estimator is indeed consistent.

$r(n)$ is an arbitrary signal For arbitrary signals it is not advised to use the estimator (2.13) because a division by a small number is possible, resulting in an estimator that won't converge. Another thing that must be considered when working with arbitrary signals is that arbitrary signals are aperiodic. If we want to get a better estimate of the FRF we will need to cut the measurement into M pieces of N samples. If the total number of samples

NM is constant, this will results in a trade-off between the frequency resolution f_s/N and noise suppression. An estimator that is used for arbitrary signals is

$$\hat{G}(\Omega_k) = \frac{\frac{1}{M}\sum_{m=0}^{M} Y^{(m)}(k)\overline{U^{(m)}(k)}}{\frac{1}{M}\sum_{m=0}^{M} U^{(m)}(k)\overline{U^{(m)}(k)}} \tag{2.14}$$

Here there is no danger for the denominator to become small. This estimator is consistent when only the output is perturbed by noise. However, in our case the input is also perturbed. Taking the limit as $M \to \infty$ gives

$$\lim_{M\to\infty} \hat{G}(\Omega_k) = \frac{\mathbb{E}\{Y^{(m)}(k)\overline{U^{(m)}(k)}\}}{\mathbb{E}\{U^{(m)}(k)\overline{U^{(m)}(k)}\}} = \frac{S_{YU}(k)}{S_{UU}(k)}$$

with S_{YU} being the cross-power spectrum between the output and input and S_{UU} being the auto-power spectrum of the input. Given that

$$\mathbb{E}\{R(k)\} = 0 \text{ and } \mathbb{E}\{|R(k)|^2\} = \sigma_r^2(k)$$

and the fact that $R(k)$ and $V(k)$ are uncorrelated we get the following result

$$\lim_{P\to\infty} \hat{G}(\Omega_k) = \frac{G(\Omega_k)\sigma_r^2(k) - \sigma_v^2(k)}{\sigma_r^2(k) + \sigma_v^2(k)} \neq G(\Omega_k)$$

Thus, the estimator (2.14) is inconsistent.

Indirect method It is possible to get around the problem of the estimator (2.14) by also using the reference signal $r(n)$. Instead of modeling the transfer function from input (u) to output (y), we will model the transfer function from reference (r) to output (y) and from reference (r) to input (u).

$$\hat{G}(\Omega_k) = \frac{\frac{1}{P}\sum_{m=0}^{P} Y^{(m)}(k)\overline{R^{(m)}(k)}}{\frac{1}{P}\sum_{m=0}^{P} U^{(m)}(k)\overline{R^{(m)}(k)}} \tag{2.15}$$

Doing some calculations brings us to

$$\lim_{M\to\infty} \hat{G}(\Omega_k) = \frac{\mathbb{E}\{Y^{(m)}(k)\overline{R^{(m)}(k)}\}}{\mathbb{E}\{U^{(m)}(k)\overline{R^{(m)}(k)}\}} = \frac{S_{YR}(k)}{S_{UR}(k)} = G(\Omega_k)$$

Thus, by keeping the reference signal and using it, it is possible to get a consistent estimate when using arbitrary excitations.

2.16 Conclusion

Multisines can be used to identify nonparametric estimates of the FRF. The robust LPM allows for the transients to be suppressed. Even if the system is in steady state, the noise transients can still deteriorate the quality of the FRF estimate. This is a reason why the robust LPM can be quite effective.

It is useful to keep the reference signal that is applied to the system. When the system is excited by an arbitrary excitation, this information can be used to get a consistent estimate of the FRF even if both the input and the output are perturbed by noise.

Finally, the authors of [2] offer MATLAB code that can perform the robust LPM for periodic and arbitrary excitations. These MATLAB function can also identify the best linear approximation of a nonlinear system. These functions can also handle MIMO systems.

Appendix

2.A Transient term

Suppose that a DT LTI system is of the following form.

$$a_0y(n) + a_1y(n-1) + a_2y(n-2) = b_0u(n) + b_1u(n-1) \tag{2.16}$$

The DFT of a sequence is actually just a windowed version of the Z-transform. To see this, the window is defined as

$$w(n) = \begin{cases} 1, & 0 \leq n < N \\ 0, & \text{otherwise} \end{cases}$$

The windowed Z-transform of a sequence $x(n)$ is then given by

$$\mathcal{Z}\{w(n)x(n)\} = \sum_{n=-\infty}^{+\infty} w(n)x(n)z^{-n} = \sum_{n=0}^{N-1} x(n)z^{-n}$$

Evaluating the expression above in $z = e^{j2\pi k/N}$ is exactly the DFT of $x(n)$.

$$\mathcal{Z}\{w(n)x(n)\}|_{z=e^{j2\pi k/N}} = \sum_{n=0}^{N-1} x(n)e^{-j2\pi kn/N} = \text{DFT}\{x(n)\}$$

Thus, taking the windowed Z-transform of both sides of (2.16) and evaluating it in $z = e^{j2\pi k/N}$ is the same as taking the DFT of both sides.

For simplicity, let's only consider one of the terms.

$$a_pw(n)y(n-p)$$

a_p is just a constant, so that can also be left out in the analysis.

$$\mathcal{Z}\{w(n)y(n-p)\} = \sum_{n=0}^{N-1} y(n-p)z^{-n}$$

After some manipulations:

$$\mathcal{Z}\{w(n)y(n-p)\} = z^{-p}\sum_{n=0}^{N-1} y(n)z^{-n} + \sum_{n=0}^{p-1}[y(n-p) - y(n-p+N)z^{-N}]z^{-n}$$

Evaluating this expression in $z = e^{j2\pi k/N}$ gives

$$\begin{aligned}\mathcal{Z}\{w(n)y(n-p)\}|_{z=e^{j2\pi k/N}} =& (e^{-j2\pi k/N})^p \sum_{n=0}^{N-1} y(n)e^{-j2\pi kn/N} \\ &+ \sum_{n=0}^{p-1}[y(n-p) - y(n-p+N)](e^{-j2\pi k/N})^n\end{aligned}$$

Note that z^{-N} disappears because $e^{-j2\pi Nn/N} = 1$. The first term contains the DFT of $y(n)$. The second term is a polynomial in $e^{-j2\pi k/N}$ that depends on $y(n-p) - y(n-p+N)$. In other words, it depends on the difference between samples from the previous period and samples from the current period.

$$\mathcal{Z}\{w(n)y(n-p)\}|_{z=e^{j2\pi k/N}} = (e^{-j2\pi k/N})^pY(k) + I_{y,p}(e^{-j2\pi k/N})$$

Applying this to (2.16) gives

$$Y(k)(\sum_{p=0}^{2} a_p(e^{-j2\pi k/N})^p) = U(k)(\sum_{p=0}^{1} b_p(e^{-j2\pi k/N})^p) + I(e^{-j2\pi k/N}) \tag{2.17}$$

with

$$I(e^{-j2\pi k/N}) = \sum_{p=0}^{1} b_p I_{u,p}(e^{-j2\pi k/N}) - \sum_{p=0}^{2} a_p I_{y,p}(e^{-j2\pi k/N}) \tag{2.18}$$

Notice that

$$G(z^{-1})|_{z=e^{j2\pi k/N}} = G(e^{-j2\pi k/N}) = \frac{B(e^{-j2\pi k/N})}{A(e^{-j2\pi k/N})} = \frac{\sum_{p=0}^{1} b_p(e^{-j2\pi k/N})^p}{\sum_{p=0}^{2} a_p(e^{-j2\pi k/N})^p}$$

Dividing (2.17) by $A(e^{-j2\pi k/N})$ then gives the final form

$$\boxed{Y(k) = G(e^{-j2\pi k/N})U(k) + T(k)} \tag{2.19}$$

with

$$T(k) = \frac{I(e^{-j2\pi k/N})}{A(e^{-j2\pi k/N})}$$

2.B DFT of white noise

A white noise sequence $v(n)$ has the following properties

$$\mathbb{E}\{v(n)\} = 0$$
$$\mathbb{E}\{v(n)v(m)\} = \sigma^2\delta(n-m)$$

The DFT of this white noise sequence is

$$V(k) = \sum_{n=0}^{N-1} v(n)e^{-j2\pi kn/N}$$

$\mathbb{E}\{V(k)\}$ The expected value of $V(k)$ is

$$\mathbb{E}\{V(k)\} = \sum_{n=0}^{N-1} \mathbb{E}\{v(n)\}e^{-j2\pi kn/N} = \sum_{n=0}^{N-1} 0e^{-j2\pi kn/N} = 0$$

$\mathbb{E}\{V(k)\overline{V(l)}\}$ The expected value of $V(k)\overline{V(l)}$ is

$$\begin{aligned}
\mathbb{E}\{V(k)\overline{V(l)}\} &= \mathbb{E}\{\sum_{n=0}^{N-1} v(n)e^{-j2\pi kn/N} \sum_{m=0}^{N-1} v(m)e^{j2\pi lm/N}\} \\
&= \sum_{n=0}^{N-1}\sum_{m=0}^{N-1} \mathbb{E}\{v(n)v(m)\}e^{-j2\pi kn/N}e^{j2\pi lm/N} \\
&= \sigma^2 \sum_{n=0}^{N-1}\sum_{m=0}^{N-1} \delta(n-m)e^{-j2\pi kn/N}e^{j2\pi lm/N} \\
&= \sigma^2 \sum_{n=0}^{N-1} e^{-j2\pi(k-l)n/N} = \begin{cases} N\sigma^2 \text{ if } \mathrm{mod}(k-l,N) = 0 \\ 0 \text{ otherwise} \end{cases}
\end{aligned}$$

When $k = l$, this result becomes

$$\mathbb{E}\{|V(k)|^2\} = N\sigma^2$$

$\mathbb{E}\{V(k)V(l)\}$ The expected value of $V(k)V(l)$ is

$$\begin{aligned}
\mathbb{E}\{V(k)V(l)\} &= \mathbb{E}\{\sum_{n=0}^{N-1} v(n)e^{-j2\pi kn/N} \sum_{m=0}^{N-1} v(m)e^{-j2\pi lm/N}\} \\
&= \sum_{n=0}^{N-1}\sum_{m=0}^{N-1} \mathbb{E}\{v(n)v(m)\}e^{-j2\pi kn/N}e^{-j2\pi lm/N} \\
&= \sigma^2 \sum_{n=0}^{N-1} e^{-j2\pi(k+l)n/N} = \begin{cases} N\sigma^2 \text{ if } \mathrm{mod}(k+l,N) = 0 \\ 0 \text{ otherwise} \end{cases}
\end{aligned}$$

When $k = l$ and $\mathrm{mod}(2k, N) \neq 0$, this result becomes

$$\mathbb{E}\{V^2(k)\} = 0$$

2.C Covariance estimation

The output spectrum in a window of size $2n$ around an excited frequency line is given by

$$Y_n = K_n\Theta + V_n$$

The least squares solution is given by

$$\hat{\Theta} = (K_n^H K_n)^{-1} K_n^H Y_n$$

A key assumption used to estimate the covariance $C_Y(kP)$ is that V_n is assumed to have a flat power spectrum in the window $2n$.

The residual is the difference between the measured spectrum and the predicted spectrum.

$$\hat{V}_n = Y_n - K_n\hat{\Theta} = (I_{2n} - K_n(K_n^H K_n)^{-1}K_n^H)Y_n = P_n Y_n$$

Using the fact that $P_n K_n = K_n - K_n = 0$ we get

$$\hat{V}_n = P_n V_n$$

Next up, we want to to see how $\hat{V}_n^H \hat{V}_n$ relates to $V_n^H V_n$.

$$\hat{V}_n^H \hat{V}_n = V_n^H P_n^H P_n V_n$$

First, it is easy to see that $P_n^H = P_n$. Next, it turns out that P_n is an idempotent matrix.

$$\begin{aligned} P_n P_n &= (I_{2n} - K_n(K_n^H K_n)^{-1}K_n^H)(I_{2n} - K_n(K_n^H K_n)^{-1}K_n^H) \\ &= I_{2n} - 2K_n(K_n^H K_n)^{-1}K_n^H + K_n(K_n^H K_n)^{-1}K_n^H = P_n \end{aligned}$$

Thus, we get

$$\hat{V}_n^H \hat{V}_n = V_n^H P_n V_n = \text{trace}(V_n^H P_n V_n) = \text{trace}(P_n V_n V_n^H) \tag{2.20}$$

In this step we used the fact that the trace of a scalar is a scalar and the fact that matrices in a trace can be circularly permuted ($\text{trace}(ABC) = \text{trace}(BCA)$). It is assumed that V_n has a flat power spectrum in the window $2n$. This means that

$$\mathbb{E}\{V_n V_n^H\} = \sigma_Y^2(kP) I_{2n}$$

Plugging this into (2.20) and taking the expected value gives

$$\mathbb{E}\{\hat{V}_n^H \hat{V}_n\} = \sigma_Y^2(kP)\text{trace}(P_n) \tag{2.21}$$

P_n is an idempotent matrix, meaning that its eigenvalues can only be 0 or 1. Additionally, because P_n and K_n are each other's orthogonal complement, the rank of P_n is related to the rank of K_n.

$$K_n P_n = 0 \Rightarrow \text{rank}(P_n) = 2n - \text{rank}(K_n)$$

If K_n is full column rank and if K_n has more rows than columns, then the rank of K_n is equal to the number of columns in K_n.

$$\text{rank}(K_n) = R + 1$$

The trace of a matrix is the sum of the eigenvalues of a matrix. The sum of the eigenvalues of P_n is exactly equal to the rank of P_n, because the rank of P_n is equal to the number of nonzero eigenvalues and because the eigenvalues can only be 0 or 1.

$$\text{trace}(P_n) = \text{rank}(P_n) = 2n - (R+1) = q^{\text{noise}}$$

Finally, this explains why $\hat{V}_n^H \hat{V}_n$ must be divided by q^{noise} to get an unbiased estimate of the covariance.

$$\boxed{\sigma_Y^2(kP) = \frac{\mathbb{E}\{\hat{V}_n^H \hat{V}_n\}}{q^{\text{noise}}}}$$

Chapter 3
Model reference control

3.1 Introduction

The first part of this chapter is a summary of the work presented in [4]. From section 3.6 and on, improvements are made to the existing methods.

3.2 Problem statement

The first assumption that is made is that $G(\Omega)$ is stable and minimum-phase. It is also possible to extend this theory to unstable nonminimum-phase systems. This will be done later in section 3.9.

The system is controlled by an unknown controller $K(\Omega, \rho)$ in closed loop (CL).

$$\mathrm{CL}(\Omega) = \frac{K(\Omega, \rho)G(\Omega)}{1 + K(\Omega, \rho)G(\Omega)}$$

$\rho = \begin{bmatrix} \rho_1 & \dots & \rho_{n_\rho} \end{bmatrix}^T$ is a vector containing the optimization parameters. In this work $K(\Omega, \rho)$ is linear in the parameters.

$$K(\Omega, \rho) = \beta(\Omega)\rho \tag{3.1}$$

with $\beta(\Omega)$ being a row vector with n_ρ elements. The idea of model reference control, is to get the closed loop system "as close" as possible to a used-defined reference system $M(\Omega)$.

$$M(\Omega) \approx \frac{K(\Omega, \rho)G(\Omega)}{1 + K(\Omega, \rho)G(\Omega)}$$

$M(\Omega)$ is assumed to be a stable causal LTI system. This criterion can be quantified by using the 2-norm of a transfer function.

$$J_{mr}(\rho) = \left|\left| F(\Omega)\left[M(\Omega) - \frac{K(\Omega, \rho)G(\Omega)}{1 + K(\Omega, \rho)G(\Omega)} \right] \right|\right|_2^2 \tag{3.2}$$

$F(\Omega)$ is a user-defined weighing filter that can be chosen to highlight specific frequencies. The 2-norm of a SISO system is defined differently for CT and DT systems. For CT systems it is

$$||H(s)||_2^2 = \frac{1}{2\pi} \int_{-\infty}^{+\infty} |H(j\omega)|^2 d\omega$$

and for DT systems it is

$$||H(z^{-1})||_2^2 = \frac{1}{2\pi} \int_{-\pi}^{\pi} |H(e^{j\omega})|^2 d\omega$$

3.3 Convex cost

One problem with the use of (3.2) as a cost function is that it is not convex. In order to solve this, we must first define the ideal controller $K^*(\Omega)$ as

$$K^*(\Omega) = \frac{M(\Omega)}{G(\Omega)(1 - M(\Omega))}$$

This definition ensures that the closed loop system is equal to the reference system by construction.

$$\frac{K^*(\Omega)G(\Omega)}{1 + K^*(\Omega)G(\Omega)} = M(\Omega)$$

Note that it is possible that K^* is not realizable i.e.

$$\nexists \rho \text{ such that } K(\Omega, \rho) = K^*(\Omega)$$

Next, both terms in (3.2) can be put under the same numerator.

$$M(\Omega) - \frac{K(\Omega, \rho)G(\Omega)}{1 + K(\Omega, \rho)G(\Omega)} = \frac{M(\Omega) - (1 - M(\Omega))K(\Omega, \rho)G(\Omega)}{1 + K(\Omega, \rho)G(\Omega)}$$

The sensitivity function is approximated by the ideal sensitivity function. The validity of this approximation should be verified afterwards.

$$\frac{1}{1 + K(\Omega, \rho)G(\Omega)} \approx \frac{1}{1 + K^*(\Omega)G(\Omega)} = \frac{1}{1 + \frac{M(\Omega)}{1 - M(\Omega)}} = 1 - M(\Omega)$$

This leads to the definition of the convex cost function.

$$\boxed{J(\rho) = \left|\left|F(\Omega)(1 - M(\Omega))\Big[M(\Omega) - (1 - M(\Omega))K(\Omega, \rho)G(\Omega)\Big]\right|\right|_2^2} \tag{3.3}$$

Of course, not all forms of $K(\Omega, \rho)$ will make this cost function convex. However, this is the case when $K(\Omega, \rho)$ is linear in the parameters (3.1). Note that the cost is minimized for the ideal controller if the ideal controller is realizable.

$$K(\rho^*, \Omega) = K^*(\Omega) \Longrightarrow J(\rho^*) = 0$$

3.4 Other cost functions

We can devise many other cost functions that solve this problem. An example is the following.

$$J_K(\rho) = ||K(\Omega, \rho) - K^*(\Omega)||_2^2$$

This cost function minimizes the square of the difference between the actual controller $K(\Omega, \rho)$ and the ideal controller $K^*(\Omega)$. If $K(\Omega, \rho)$ is linear in the parameters, then this is just simple least squares regression. However, this is not the same as optimizing ρ to the cost function (3.3) and will result in a different outcome. This shows that the choice of the cost function is an important part of optimization and must be done with care.

3.5 Correlation-based approach

As $G(\Omega)$ is not known in (3.3), the authors of [4] propose the correlation-based approach. They give algorithms for periodic and arbitrary excitations. Here we will focus on their equations concerning periodic excitations. We will also restrict this section to DT systems ($\Omega = z^{-1}$), as they have done in their paper.

One thing to note, is that all the equations in [4] are written in the TD. These will be translated to the FD in section 3.6. The reader is recommended to not to spend too much time trying to understand the definitions in this section as they will make more sense in the next section.

Model First it is assumed that the output of the DT system is perturbed by some noise $v(n)$.

$$y(n) = G(q^{-1})u(n) + v(n) \tag{3.4}$$

with q^{-1} being the backshift operator: $q^{-1}x(n) = x(n-1)$. N denotes the period of the input.

$$u(n) = u(n+N) \tag{3.5}$$

The additive noise is modelled as DT filtered white noise.

$$v(n) = S_v(q^{-1})e_v(n)\,, e_v(n) \text{ with } \mathbb{E}\{e_v(n)\} = 0 \text{ and } \mathbb{E}\{e_v(n)^2\} = \sigma^2$$

Error signal Then a new quantity $\epsilon(n, \rho)$ is defined [4, eq. (15)].

$$\begin{aligned}\epsilon(n,\rho) &= M(q^{-1})u(n) - K(q^{-1},\rho)(1 - M(q^{-1}))y(n)\\ &= [M - K(\rho)(1-M)G]u(n) - K(\rho)(1-M)S_v e_v(n)\end{aligned}$$

In the second row the operators q^{-1} are left out for clarity.

Input filtering Additionally, the filter W is defined [4, eq. (41)]

$$W(e^{-j\omega_k}) = \frac{F(e^{-j\omega_k})(1 - M(e^{-j\omega_k}))}{S_{UU}(e^{-j\omega_k})}$$
$$\omega_k = \frac{2\pi k}{N}\,, \quad k = 0, \ldots, N-1$$

$S_{UU}(e^{-j\omega_k})$ is the discrete Fourier transform (DFT) of the autocorrelation of u(n) [4, eqs. (38) and (39)].

$$R_{uu}(\tau) = \frac{1}{N}\sum_{n=0}^{N-1} u(n-\tau)u(n) \tag{3.6}$$

$$S_{UU}(e^{-j\omega_k}) = \sum_{\tau=0}^{N-1} R_{uu}(\tau)e^{-j\tau\omega_k} \tag{3.7}$$

If the system is in steady state, $u(n-\tau)$ is known for negative time indices by using (3.5). If the experiment starts with zero initial conditions, then $u(n-\tau) = 0$ for $n - \tau \leq 0$.

The filter W is applied on the input $u(n)$. As is remarked at the end of [4, Sec. 4.4], if a parametric representation of $S_{UU}(q^{-1})$ is known, this filter can be applied in the TD.

$$u_W(n) = W(q^{-1})u(n)$$

Note that this can be problematic if $S_{UU}(q^{-1})$ has zeros that are not on the unit circle, as the filter $W(q^{-1})$ will then be unstable. More information concerning this is given in appendix 3.A.

Correlation criterion Then, the crosscorrelation between between $u_W(n)$ and $\epsilon(n,\rho)$ is calculated.

$$R_{u_W\epsilon}(\tau,\rho) = \frac{1}{NP}\sum_{n=0}^{NP-1} u_W(n-\tau)\epsilon(n,\rho) \tag{3.8}$$

with P being the number of periods measured. Note that as in (3.6), $u_W(n-\tau)$ can be found by using (3.5) if the system is in steady state. If the system starts off in zero initial conditions, $u_W(n-\tau) = 0$ for $n-\tau \leq 0$.

The correlation criterion $J_{NP,l_1}(\rho)$ can then be defined.

$$\boxed{J_{NP,l_1}(\rho) = \sum_{\tau=-l_1}^{l_1} R^2_{u_W\epsilon}(\tau,\rho)} \tag{3.9}$$

with $l_1 \leq N/2$ being a parameter that can be chosen by the user. The idea behind this parameter l_1 is discussed in detail in section 3.7. It is then proven in [4, Appendix II] that (3.9) converges to (3.3) for $N, P \to \infty$ with probability 1 under certain conditions.

$$\lim_{N,P\to\infty} J_{NP,l_1}(\rho) = J(\rho)\,, \text{ w.p. } 1$$

However, for finite data, it is proven that the estimator is biased [4, eq. (37)]

$$\mathbb{E}\{J_{NP,l_1}(\rho)\} \approx \tilde{J}_{NP,l_1}(\rho) + \frac{\sigma^2(2l_1+1)}{2\pi NP}\int_{-\pi}^{\pi} \frac{|1-M|^4|K(\rho)|^2|S_v|^2|F|^2}{S_{UU}(e^{-j\omega})}d\omega \tag{3.10}$$

with $\tilde{J}_{NP,l_1}(\rho)$ being the control criterion in the absence of noise. A proof of this is given in section 3.8.

3.6 Translation to frequency domain

In this section the results from the previous section will be translated to the FD. Here we will show that a nonparametric estimate of the system $G(\Omega)$ is actually hidden in the mathematics. Thus, even though the parametric modeling step is skipped, there is still a nonparametric model.

3.6.1 Disadvantages of TD

There are some disadvantages to working in the TD. Here are some that are relevant to this subject.

- TD filtering can only be done easily if the underlying system is a DT system.
- The filtering of $u(n)$ with $W(q^{-1})$ can only be performed in the TD if a parametric representation of $S_{UU}(q^{-1})$ is known and if $S_{UU}(q^{-1})$ only has zeros on the unit circle. (see appendix 3.A).
- If the system starts out with zero initial conditions or in steady state, then the transient response can be taken into account, as knowledge of the input and output signals are known before they are applied. This makes it possible to calculate (3.6) and (3.8) for $n-\tau \leq 0$. However, if the system does not start with zero initial conditions or in steady state, this approach will not work and the transient term will not be suppressed.

These problems can be solved by working in the FD. To address the first point: FD methods can also handle CT systems. For the second point: a convolution in the TD can explode when the system is unstable. However, this is not a problem in the FD as a convolution is the TD becomes a simple multiplication in the FD. Finally, for the third point: the robust LPM (see section 2.14) is able to estimate a non-parametric estimate of the frequency response function (FRF) from noisy input-output data, while suppressing the transient term.

3.6.2 Nonparametric estimate

By translating the formulas of section 3.5 to the FD, it will become immediately apparent that a nonparametric estimate is being calculated. The first step in translating the problem from the TD to the FD is to use Parseval's theorem. According to Parseval's theorem, the sum of squares in the TD is equivalent to the sum of the norms squared in the FD. The cost function (3.9) represents a sum of squares in the TD. Parseval's theorem will be discussed in greater detail in section 3.7.

Now, instead of calculating $\epsilon(n, \rho)$ in the TD, it can be calculated in the FD. Note that this also makes the computations less intensive, as a convolution in the TD becomes a multiplication in the FD. As the input to the system is assumed to be periodic, the frequencies Ω_k will correspond to the DFT bins kP.

$$E(kP, \rho) = M(\Omega_k)U(kP) - K(\Omega_k, \rho)(1 - M(\Omega_k))Y(kP)$$

Applying the filter W on $u(n)$ can also be done in the FD.

$$U_W(kP) = W(\Omega_k)U(kP)$$

with

$$W(\Omega_k) = \frac{F(\Omega_k)(1 - M(\Omega_k))}{U(kP)\overline{U(kP)}}$$

The denominator $U(kP)\overline{U(kP)}$ represents the auto-power spectrum of the input $S_{UU}(e^{-j\omega_k})$.[1] This equivalence is proven in appendix 3.B. Then, the cross-power spectrum between $\epsilon(n, \rho)$ and $u_W(n)$ is also calculated in the FD by doing a simple multiplication.

$$S_{U_W E}(\Omega_k, \rho) = U_W(kP)\overline{E(kP, \rho)} \tag{3.11}$$

Expanding (3.11) makes the link to the cost function (3.3) immediately apparent.

$$S_{U_W E}(\Omega_k, \rho) = U(kP)\frac{F(1 - M)}{U(kP)\overline{U(kP)}}\overline{MU(kP) - K(\rho)(1 - M)Y(kP)} \tag{3.12}$$

$$= F(1 - M)\overline{M - K(\rho)(1 - M)\hat{G}(\Omega_k)} \tag{3.13}$$

with

$$\hat{G}(\Omega_k) = \frac{Y(kP)\overline{U(kP)}}{U(kP)\overline{U(kP)}} = \frac{Y(kP)}{U(kP)} \tag{3.14}$$

The index Ω_k was left out in F, M and K for clarity. $\hat{G}(\Omega_k)$ is a non-parametric estimate of the system. If $\hat{G}$ is replaced by the actual system G, then $S_{U_W E}(\Omega_k, \rho)$ is exactly the quantity being integrated over in (3.3).

[1] Actually $U(kP)\overline{U(kP)}$ corresponds to $NS_{UU}(e^{-j\omega_k})$. This proportionality constant is left out because it will appear in both the numerator and the denominator.

Thus, a non-parametric estimate of the system $\hat{G}$ can be found, followed by calculating the cost function in the FD.

$$\boxed{J_N(\rho) = \sum_{k \in \mathrm{K_{exc}}} \Big| H(\Omega_k, \rho) \Big|^2} \tag{3.15}$$

with $\mathrm{K_{exc}}$ being the set of excited DFT bins and

$$H(\Omega_k, \rho) = F(\Omega_k)(1 - M(\Omega_k)) \Big[M(\Omega_k) - (1 - M(\Omega_k)) K(\Omega_k, \rho) \hat{G}(\Omega_k) \Big] \tag{3.16}$$

By working like this, we can be much more flexible with the manner in which we estimate the FRF nonparametrically. Let's take a closer look at the nonparametric estimator that is hidden inside the formulas of the TD.

$$\hat{G}(\Omega_k) = \frac{Y(kP)}{U(kP)}$$

Now, let's separate $y(n)$ into its P periods $y^{(p)}(n)$.

$$y^{(p)}(n) = y(n + pP)\,, \quad p = 0, \ldots, P-1$$

We can also define the DFT for every one of the periods.

$$Y^{(p)}(k) = \sum_{n=0}^{N-1} y^{(p)}(n) e^{-j2\pi kn/N}\,, \quad p = 0, \ldots, P-1$$

With these definitions we can get a better understanding of what $Y(kP)$ represents.

$$\begin{aligned} Y(kP) &= \sum_{n=0}^{NP-1} y(n) e^{-j2\pi (kP) n/(NP)} \\ &= \sum_{p=0}^{P-1} \sum_{n=0}^{N-1} y(n + pP) e^{-j2\pi kn/N} = \sum_{p=0}^{P-1} Y^{(p)}(k) \end{aligned}$$

Thus, the nonparametric estimate becomes

$$\hat{G}(\Omega_k) = \frac{\frac{1}{P} \sum_{p=0}^{P-1} Y^{(p)}(k)}{\frac{1}{P} \sum_{p=0}^{P-1} U^{(p)}(k)}$$

This is a consistent estimator for the model (3.4). Indeed, if we translate (3.4) to the FD we obtain

$$Y^{(p)}(k) = G(\Omega_k) U^{(p)}(k) + V^{(p)}(k)\,, \quad p = 0, \ldots, P-1$$

Given that the input is periodic $U^{(p)}(k) = U_0(k)$, we get

$$\hat{G}(\Omega_k) = \frac{\frac{1}{P} \sum_{p=0}^{P-1} \Big[G(\Omega_k) U_0(k) + V^{(p)}(k) \Big]}{U_0(k)} = G(\Omega_k) + \frac{1}{U_0(k)} \frac{1}{P} \sum_{p=0}^{P-1} V^{(p)}(k)$$

The output noise is assumed to be white, which means that $\mathbb{E}\{V(k)\} = 0$. Taking the limit for $P \to \infty$ gives

$$\lim_{P \to \infty} \hat{G}(\Omega_k) = G(\Omega_k) + \frac{1}{U_0(k)} \mathbb{E}\{V(k)\} = G(\Omega_k)$$

The law of large numbers for independent experiments is used in the first equation. The estimator is also consistent if the measurement of the input is noisy.

$$U^{(p)} = U_0(k) + N_U^{(p)}(k)$$

3.7 Parseval's theorem

Parseval's theorem is very simple: the energy of the signal in the TD is the same as the energy of the signal in the FD.

$$\sum_{n=0}^{N-1} x(n)^2 = \frac{1}{N} \sum_{k=0}^{N-1} |X(k)|^2 \tag{3.17}$$

with $X(k) = \text{DFT}\{x(n)\}$. The factor $1/N$ is specific to the definition of the DFT that is used in this work and will be different if another definition is used.

The cost function in the FD (3.15) is also the sum of squares.

$$J_N(\rho) = \sum_{k=0}^{N-1} |H(\Omega_k, \rho)|^2$$

According to Parseval's theorem, the above sum is equivalent to a sum of squares in the TD.

$$J_N(\rho) = N \sum_{n=0}^{N-1} h(n, \rho)^2$$

with $h(n, \rho)$ being the IDFT of $H(\Omega_k, \rho)$. If $N \to \infty$, $h(n, \rho)$ is the impulse response of the system $H(\Omega, \rho)$. The trick that the authors use in [4] is the fact that the impulse response of a non-minimum phase system will fade away after some time.

$$\exists l_1 \text{ such that } h(n) \approx 0 \text{ for } n > l_1$$

Applying this approximation to the cost function gives

$$J_N(\rho) \approx N \sum_{n=0}^{l_1} h(n, \rho)^2 \tag{3.18}$$

Example Let's take a very simple first order system.

$$H(z^{-1}) = \frac{0.2z^{-1}}{1 - 0.8z^{-1}} \tag{3.19}$$

The impulse response of this system for the first 51 samples is plotted in figure 3.7.1. Additionally, the red dotted line shows the impulse response with a bit of additive Gaussian white noise.

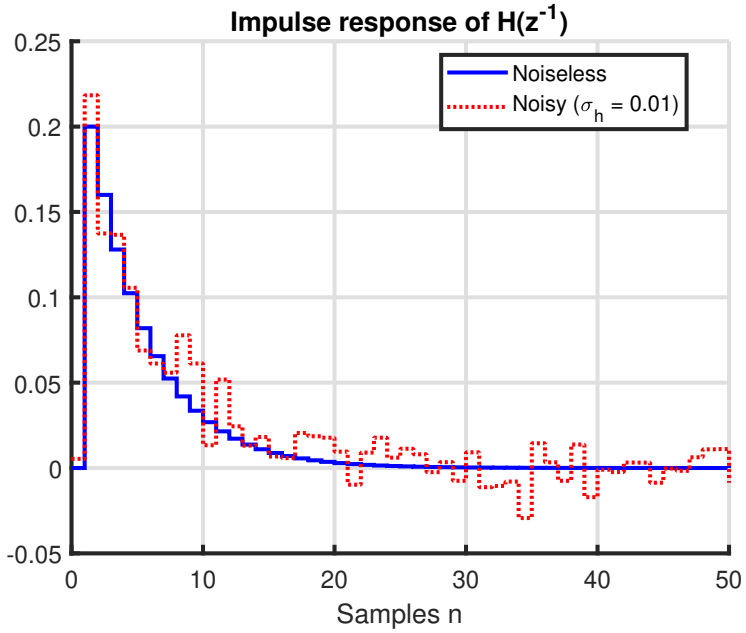

Figure 3.7.1 – Impulse response of (3.19) with and without additive Gaussian white noise.

The approximate energy of the signal in the TD $\sum_{n=0}^{l_1} h(n,\rho)^2$ is plotted in figure 3.7.2 (blue full line). It quickly converges to the energy of the signal in the FD $\frac{1}{51}\sum_{k=0}^{50}|H(k)|^2$. This is also the case for the noisy signal (dotted red line); it converges to its energy in the FD. Ideally however, we would like the energy is the noisy case to be as close to the actual, noiseless energy. This is not the case; there is a certain bias. In this case, taking $l_1 = 10$, would result in less bias, while still keeping the information that is needed. This can also be seen in figure 3.7.1: the impulse response after $n = 10$ is at or below noise level. Thus the impulse response after $n = 10$ does not contain much useful information and will only contribute to a biased cost function.

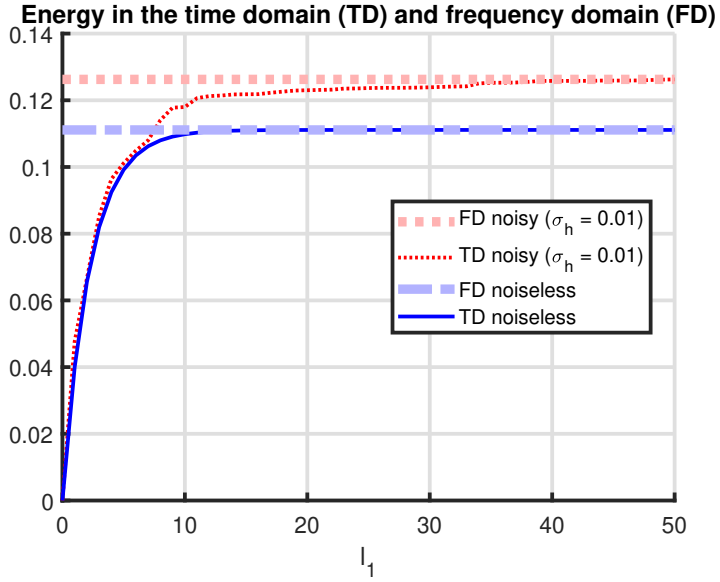

Figure 3.7.2 – Energy of the signal in the TD and the FD (divided by N).

In [4], l_1 has a slightly different interpretation. As can be seen in (3.8), the sum goes from $-l_1$ to l_1. This is because the sum is taken over the crosscorrelation of u_W and ϵ. The crosscorrelation is symmetric, which is why the sum also extends into negative values of τ. The impulse response is not symmetric which is why the sum starts at $n = 0$ in (3.18).

3.8 Bias

Let's quantify the bias that was discussed in the previous section. The results will be very close to (3.10). Let's assume that the input is a periodic signal that is excited at all the DFT frequencies. The output is perturbed by filtered white noise.

$$Y^{(p)}(k) = G(\Omega_k)U_0(k) + S_v(\Omega_k)V^{(p)}(k)$$

with $\mathbb{E}\{V^{(p)}(k)\} = 0$ and $\mathbb{E}\{|V^{(p)}(k)|^2\} = N\sigma^2$. The nonparametric estimate of the FRF is

$$\hat{G}(\Omega_k) = \frac{\frac{1}{P}\sum_{p=0}^{P-1} Y^{(p)}(k)}{\frac{1}{P}\sum_{p=0}^{P-1} U^{(p)}(k)} = G(\Omega_k) + \frac{1}{U_0(k)}\frac{1}{P}\sum_{p=0}^{P-1} S_v(\Omega_k)V^{(p)}(k)$$

The statistical properties of this estimator are

$$\begin{aligned}
\mathbb{E}\{\hat{G}(\Omega_k)\} &= G(\Omega_k) \\
\mathbb{E}\{|\hat{G}(\Omega_k)|^2\} &= |G(\Omega_k)|^2 + \frac{1}{|U_0(k)|^2}\frac{|S_v(\Omega_k)|^2 N\sigma^2}{P} \\
&= |G(\Omega_k)|^2 + \frac{1}{NP}\frac{|S_v(\Omega_k)|^2\sigma^2}{|U_0(k)/N|^2}
\end{aligned}$$

$|S_v(\Omega_k)|^2\sigma^2$ quantifies the power of the noise at the k-th DFT bin and $|U_0(k)/N|$ quantifies the energy of the signal at the k-th bin. This becomes evident when the RMS of the signals is calculated.

$$\mathrm{RMS}^2 = \frac{1}{N}\sum_{n=0}^{N-1} x(n)^2 = \sum_{k=0}^{N-1}\left|\frac{X(k)}{N}\right|^2$$

Thus, $\frac{|S_v(\Omega_k)|^2\sigma^2}{|U_0(k)/N|^2}$ is the noise-to-signal ratio at the k-th DFT bin.

Now we have all the information we need to calculate the expected value of the cost function.

$$J_N(\rho) = \sum_{k=0}^{N-1}|H(\Omega_k,\rho)|^2 = \sum_{k=0}^{N-1}\left|F(\Omega_k)(1-M(\Omega_k))\Big[M(\Omega_k) - (1-M(\Omega_k))K(\Omega_k,\rho)\hat{G}(\Omega_k)\Big]\right|^2$$

Taking the expected value gives

$$\begin{aligned}
\mathbb{E}\{J_N(\rho)\} &= \sum_{k=0}^{N-1}\left|F(\Omega_k)(1-M(\Omega_k))\Big[M(\Omega_k) - (1-M(\Omega_k))K(\Omega_k,\rho)G(\Omega_k)\Big]\right|^2 \\
&\quad + \sum_{k=0}^{N-1}\frac{1}{NP}\frac{|S_v(\Omega_k)|^2\sigma^2}{|U_0(k)/N|^2}\left|F(\Omega_k)(1-M(\Omega_k))^2K(\Omega_k,\rho)\right|^2 \\
&= \tilde{J}_N(\rho) + \frac{\sigma^2}{NP}\sum_{k=0}^{N-1}\frac{|F(\Omega_k)|^2|1-M(\Omega_k)|^4|K(\Omega_k,\rho)|^2}{\mathrm{SNR}(k)}
\end{aligned}$$

with $\tilde{J}(\rho)$ being the cost function in the noiseless case and $\mathrm{SNR}(k) = \frac{|U_0(k)/N|^2}{|S_v(\Omega_k)|^2\sigma^2}$.

What if we now transform $H(\Omega_k,\rho)$ to the TD using the IDFT and approximate the cost function by only summing until l_1?

$$J_N(\rho) = \sum_{k=0}^{N-1}|H(\Omega_k,\rho)|^2 = N\sum_{k=0}^{N-1}h(n,\rho)^2 \approx N\sum_{k=0}^{l_1}h(n,\rho)^2 = J_{N,l_1}(\rho)$$

Because the sum only contains (l_1+1) noisy terms, the bias will be smaller than when the full sum is taken. To be more specific, the bias will be a factor $(l_1+1)/N$ smaller. Thus the expected value of the approximate cost function becomes

$$\boxed{\mathbb{E}\{J_{N,l_1}(\rho)\} \approx \tilde{J}_N(\rho) + \frac{\sigma^2}{NP}\frac{l_1+1}{N}\sum_{k=0}^{N-1}\frac{|F(\Omega_k)|^2|1-M(\Omega_k)|^4|K(\Omega_k,\rho)|^2}{\mathrm{SNR}(k)}} \tag{3.20}$$

If we work with DT systems $\Omega_k = e^{-j2\pi k/N}$. Taking the limit as $N \to \infty$ turns the sum into an integral.

$$\sum_{k=0}^{N-1} \frac{|F(e^{-j2\pi k/N})|^2 |1 - M(e^{-j2\pi k/N})|^4 |K(e^{-j2\pi k/N}, \rho)|^2}{\mathrm{SNR}(e^{-j2\pi k/N})} \frac{2\pi}{N} \frac{N}{2\pi}$$
$$\xrightarrow[N\to\infty]{} \frac{N}{2\pi} \int_{-\pi}^{\pi} \frac{|F(e^{j\omega})|^2 |1 - M(e^{j\omega})|^4 |K(e^{j\omega}, \rho)|^2 |S_v(e^{j\omega})|^2}{|U_0(e^{j\omega})/N|^2} d\omega$$

Inserting this into (3.20) gives

$$\boxed{\mathbb{E}\{J_{N,l_1}(\rho)\} \approx \tilde{J}(\rho) + \frac{\sigma^2(l_1+1)}{2\pi NP} \int_{-\pi}^{\pi} \frac{|F(e^{j\omega})|^2 |1 - M(e^{j\omega})|^4 |K(e^{j\omega}, \rho)|^2 |S_v(e^{j\omega})|^2}{|U_0(e^{j\omega})/N|^2} d\omega \text{ as } N \to \infty} \tag{3.21}$$

Because the sum becomes an integral, $\tilde{J}(\rho)$ actually represents the original cost function (3.3). Using the fact that $S_{UU}(e^{-j\omega}) = |U_0(e^{j\omega})/\sqrt{N}|^2$, (3.21) is almost the same as (3.10). The first difference is that the numerator contains $(l_1 + 1)$ instead of $(2l_1 + 1)$. This is due to the fact that l_1 has a slightly different interpretation as discussed before. The second difference is that N will not be present anymore in the denominator. However, this is to be expected as we are comparing the sum of the squares in the FD to the sum of the squares in the TD. According to (3.17), we must divide the sum of the squares in the FD by N in order to have a fair comparison.

$$\frac{\mathbb{E}\{J_{N,l_1}(\rho)\}}{N} \approx \frac{\tilde{J}(\rho)}{N} + \frac{\sigma^2(l_1+1)}{2\pi NP} \int_{-\pi}^{\pi} \frac{|F(e^{j\omega})|^2 |1 - M(e^{j\omega})|^4 |K(e^{j\omega}, \rho)|^2 |S_v(e^{j\omega})|^2}{S_{UU}(e^{-j\omega})} d\omega \text{ as } N \to \infty$$

3.9 Unstable systems

Open loop experiments are not practical on unstable systems. If we want to measure the FRF of an unstable system, it will have to be done in closed loop with a stabilizing controller. As discussed in section 2.15.3, the danger here is that process noise on the output will be fed back to the input. Not taking the right precautions will lead to an inconsistent nonparametric estimate of the FRF in some cases.

First, a quick summary of the solution given in [4] will be discussed. Then it will be shown that a nonparametric estimate of the FRF is again hidden in the maths.

3.9.1 Correlation-based approach

Model The setup shown in figure 3.9.1 is considered. An unstable system $G(q^{-1})$ is stabilized by a controller $K_s(q^{-1})$ in negative feedback. The reference signal $r(n)$ is entered between the controller and the system. The reference signal is assumed to be periodic. The input to the system is $u(n)$ and the output of the system $y(n)$ is perturbed by process noise $v(n)$. The closed loop TF is

$$M_s(q^{-1}) = \frac{K_s(q^{-1})G(q^{-1})}{1 + K_s(q^{-1})G(q^{-1})}$$

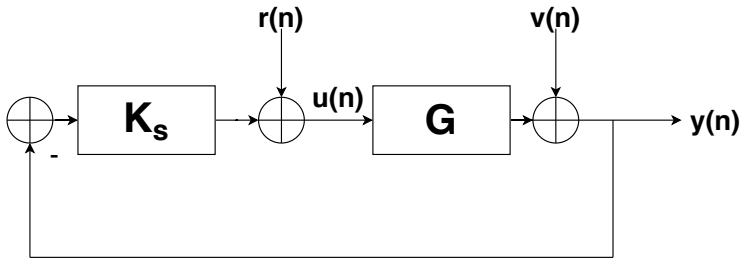

Figure 3.9.1 – Unstable LTI system with a stabilizing controller in feedback.

Error signal The error signal is the same as in section 3.5.

$$\epsilon(n, \rho) = Mu(n) - K(\rho)(1 - M)y(n)$$

Reference filtering This time, the reference signal $r(n)$ is filtered instead of the input to the system $u(n)$. The filter $W(q^{-1})$ which is used to obtain $r_W(n)$ is defined differently this time.

$$W(e^{-j\omega}) = \frac{F(e^{-j\omega})(1 - M(e^{-j\omega}))}{(1 - M_s(e^{-j\omega}))S_{RR}(e^{-j\omega})} \tag{3.22}$$

with $S_{RR}(e^{-j\omega})$ being the auto-power spectrum of the reference signal. It is pointed out in [4] that $W(e^{-j\omega})$ cannot be implemented in this way, because M_s is not known as we don't have access to a parametric representation of G. This is solved in the following way. First, $u(n)$ is written as a function of $r(n)$ and $v(n)$.

$$u(n) = \frac{1}{1 + K_sG}r(n) - \frac{K_s}{1 + K_sG}v(n)$$

Assuming that there is no noise $v(n) = 0$ and rewriting $1 + K_sG$ in terms of M_s gives

$$u(n) = (1 - M_s)r(n)$$

Thus there is a relation between the auto-power spectrum of $r(n)$ and the cross-power spectrum between $r(n)$ and $u(n)$.

$$S_{RU}(e^{-j\omega}) = (1 - M_s(e^{-j\omega}))S_{RR}(e^{-j\omega})$$

And so (3.22) becomes

$$W(e^{-j\omega}) = \frac{F(e^{-j\omega})(1 - M(e^{-j\omega}))}{S_{RU}(e^{-j\omega})}$$

$S_{RU}(e^{-j\omega})$ can be estimated from the data and the filter can be applied on $r(n)$ in the FD to obtain $r_W(n)$.

Correlation criterion Then, the crosscorrelation between between $r_W(n)$ and $\epsilon(n, \rho)$ is calculated.

$$R_{r_W\epsilon}(\tau, \rho) = \frac{1}{NP} \sum_{n=0}^{NP-1} r_W(n - \tau)\epsilon(n, \rho)$$

with P being the number of periods measured. The cost function can then be calculated by using (3.9).

3.9.2 Nonparametric estimate

The error signal in the FD becomes

$$E(kP, \rho) = M(\Omega_k)U(kP) - K(\Omega_k, \rho)(1 - M(\Omega_k))Y(kP)$$

Here, because the reference signal is periodic, the frequencies Ω_k correspond to the DFT bins kP. For the rest of this section, the frequencies Ω_k will be left out from the equations for clarity. The filtered reference signal becomes

$$R_W(kP) = \frac{F(1 - M)R(kP)}{R(kP)\overline{U(kP)}}$$

Then the cross-power spectrum between $\epsilon(n, \rho)$ and $r_W(n)$ is

$$\begin{aligned} S_{R_WE}(\Omega_k, \rho) = R_W(kP)\overline{E(kP, \rho)} &= F(1 - M)\overline{\Big[M\frac{U(kP)\overline{R(kP)}}{U(kP)\overline{R(kP)}} - K(\rho)(1 - M)\frac{Y(kP)\overline{R(kP)}}{U(kP)\overline{R(kP)}}\Big]} \\ &= F(1 - M)\overline{[M - K(\rho)(1 - M)\hat{G}(\Omega_k)]} \end{aligned}$$

with

$$\hat{G}(\Omega_k) = \frac{Y(kP)\overline{R(kP)}}{U(kP)\overline{R(kP)}} = \frac{Y(kP)}{U(kP)} \tag{3.23}$$

If $\hat{G}$ is replaced by the actual system G, $S_{R_WE}(\Omega_k, \rho)$ is exactly the quantity being integrated over in (3.3). As was discussed in section 3.5, (3.23) is equivalent to taking the DFT of every period and taking the mean of the spectra over the periods.

$$\hat{G}(\Omega_k) = \frac{\frac{1}{P}\sum_{p=0}^{P-1} Y^{(p)}(k)}{\frac{1}{P}\sum_{p=0}^{P-1} U^{(p)}(k)}$$

Note that this formula is consistent when the excitation is periodic. For arbitrary excitations it is inconsistent. It is interesting to see that the unsimplified fraction in (3.23) looks like the indirect method for estimating the FRF (see section 2.15.3).

$$\hat{G}(\Omega_k) = \frac{\frac{1}{P}\sum_{m=0}^{P} Y^{(m)}(k)\overline{R^{(m)}(k)}}{\frac{1}{P}\sum_{m=0}^{P} U^{(m)}(k)\overline{R^{(m)}(k)}}$$

This FRF estimate is consistent when using arbitrary excitations.

3.10 Weighted nonlinear least squares

It is possible to reduce the bias by using a weighted cost function. The weighing will be based on the variance of the FRF estimate.

$$\sigma^2_{\hat{G}}(\Omega_k) = \mathbb{E}\{|\hat{G}(\Omega_k) - \mathbb{E}\{\hat{G}(\Omega_k)\}|^2\}$$

The robust LPM can estimate the variance of the FRF estimate $\hat{\sigma}^2_{\hat{G}}$ for systems excited with periodic inputs. The weighted nonlinear least squares cost function is

$$J_{\text{WNLS}} = \sum_{k \in \text{K}_{\text{exc}}} \frac{|H(\Omega_k, \rho)|^2}{\hat{\sigma}^2_H(\Omega_k, \rho)} \tag{3.24}$$

with K_{exc} being the set of excited DFT bins and

$$H(\Omega_k, \rho) = F(\Omega_k)(1 - M(\Omega_k))\Big[M(\Omega_k) - (1 - M(\Omega_k))K(\Omega_k, \rho)\hat{G}(\Omega_k)\Big]$$

and

$$\hat{\sigma}^2_H(\Omega_k, \rho) = \hat{\sigma}^2_{\hat{G}}(\Omega_k)\Big|F(\Omega_k)(1 - M(\Omega_k))^2 K(\Omega_k, \rho)\Big|^2$$

The cost function (3.24) is not convex anymore as the denominator also depends on the optimization parameters ρ. Thus, the minimization of this cost function cannot be solved with convex optimization. It can be solved with the Gauss-Newton algorithm. An initial estimate of ρ can be found by minimizing the convex cost function (3.15).

3.11 Simulations

3.12 Conclusion

Appendix

3.A Division by auto-power spectrum

In section 3.5, the following filter is defined.

$$W(q^{-1}) = \frac{F(q^{-1})(1 - M(q^{-1}))}{S_{UU}(q^{-1})}$$

with $S_{UU}(q^{-1})$ being a parametric representation of the auto-power spectrum of $u(n)$.

If $u(n)$ is DT filtered white noise $u(n) = S_u(q^{-1})e_u(n)$ and a parametric representation of $S_u(q^{-1})$ is known, then the auto-power spectrum of $u(n)$ becomes

$$S_{UU}(q^{-1}) = S_u(q^{-1})S_u(q)$$

The zeros of $S_u(q^{-1})$ and $S_u(q)$ have an inverse relationship. If a is a zero of $S_u(q^{-1})$, then a^{-1} is a zero of $S_u(q)$. These zeros then become poles of $W(q^{-1})$. Thus, if $S_u(q^{-1})$ contains zeros that are not on the unit circle, the filter $W(q^{-1})$ will be unstable. And so, applying the filter in the time domain is in general not possible.

3.B DFT of crosscorrelation

The circular crosscorrelation of two discrete signals x and y is defined by [5, eq. (2.22)]

$$R_{xy}(\tau) = \sum_{n=0}^{N-1} \overline{x(n)} y(\mathrm{mod}(n+\tau, N)) \tag{3.25}$$

Taking the DFT of (3.25) gives

$$\begin{aligned} S_{XY}(k) &= \sum_{\tau=0}^{N-1} R_{xy}(\tau) e^{-j2\pi k\tau/N} = \sum_{\tau=0}^{N-1}\sum_{n=0}^{N-1} \overline{x(n)} y(\mathrm{mod}(n+\tau, N)) e^{-j2\pi k\tau/N} \\ &= \sum_{n=0}^{N-1} \overline{x(n)} \sum_{\tau=0}^{N-1} y(\mathrm{mod}(n+\tau, N)) e^{-j2\pi k\tau/N} \\ &= \sum_{n=0}^{N-1} \overline{x(n)} e^{j2\pi kt/N} \sum_{\tau=0}^{N-1} y(\mathrm{mod}(n+\tau, N)) e^{-j2\pi k(n+\tau)/N} \end{aligned}$$

The second sum is actually independent of n.

$$\begin{aligned} \sum_{\tau=0}^{N-1} y(\mathrm{mod}(n+\tau, N)) e^{-j2\pi k(n+\tau)/N} &= \sum_{\tau=0}^{N-t-1} y(n+\tau) e^{-j2\pi k(n+\tau)/N} \\ &+ \sum_{\tau=N-t}^{N-1} y(n+\tau-N) e^{-j2\pi k(n+\tau)/N} \\ &= \sum_{\tau=0}^{N-t-1} y(n+\tau) e^{-j2\pi k(n+\tau)/N} \\ &+ \sum_{\tau=-t}^{-1} y(n+\tau) e^{-j2\pi k(n+\tau+N)/N} \\ &= \sum_{\tau=-t}^{N-t-1} y(n+\tau) e^{-j2\pi k(n+\tau)/N} \end{aligned}$$

In the last step we used the fact that $e^{-j2\pi k(n+\tau+N)/N} = e^{-j2\pi k(n+\tau)/N}$. Now by doing one last substitution we get

$$\sum_{\tau=0}^{N-1} y(\mathrm{mod}(n+\tau, N)) e^{-j2\pi k(n+\tau)/N} = \sum_{\tau=0}^{N-1} y(\tau) e^{-j2\pi k\tau/N}$$

Finally, the DFT of the crosscorrelation is

$$\begin{aligned} S_{XY}(k) &= \overline{\sum_{n=0}^{N-1} x(n) e^{-j2\pi kt/N}} \sum_{\tau=0}^{N-1} y(\tau) e^{-j2\pi k\tau/N} \\ \Rightarrow S_{XY}(k) &= \overline{X(k)} Y(k) \end{aligned}$$

Chapter 4
Guaranteed stability

Bibliography

[1] Pintelon R. Lecture notes of Identification of Dynamical Systems. VUB; 2019. Can be obtained from https://vubirelec.be/knowledge/downloads/course-material.

[2] Pintelon R, Schoukens J. System identification : a frequency domain approach. 2nd ed. Hoboken, N.J.: John Wiley & Sons Inc.; 2012.

[3] Markovsky I. Low Rank Approximation: Algorithms, Implementation, Applications. Springer; 2012. Available from: http://homepages.vub.ac.be/~imarkovs/book.html.

[4] van Heusden K, Karimi A, Bonvin D. Data-driven model reference control with asymptotically guaranteed stability. International Journal of Adaptive Control and Signal Processing. 2011;25(4):331–351. Available from: https://onlinelibrary.wiley.com/doi/abs/10.1002/acs.1212.

[5] Wang C. Kernel learning for visual perception. Nanyang Technological University; 2019. Available from: https://doi.org/10.32657/10220/47835.